

Identifying the Change in Heat Vulnerability and Land-use Influence

A 20-year spatial-temporal analysis of thermal and land-use change in Fairfield and New Haven Counties, CT.

October 13, 2021

Mariana B. Alfonso Fragomeni, Ph.D., M.E.P.D.

Tracey Miller, Ph.D. Student, M.L.A.

Katherine Day, Undergraduate Assistant

Department of Plant Science and Landscape Architecture



Connecticut Institute for Resilience
and Climate Adaptation



UCONN
UNIVERSITY OF CONNECTICUT

Project support comes from the Connecticut Institute for Resilience and Climate Adaptation (CIRCA). CIRCA's mission is to increase the resilience and sustainability of communities vulnerable to the growing impacts of climate change on the natural, built, and human environments. Funding for this project was provided by the United States Department of Housing and Urban Development through the Community Development Block Grant National Disaster Recovery Program, as administered by the State of Connecticut, Department of Housing (DOH). This publication does not express the views of DOH or the State of Connecticut. The views and opinions expressed are those of the authors.

Identifying the Change in Heat Vulnerability and Land-use Influence for the Resilient Connecticut Project

Mariana B. Alfonso Fragomeni, Ph.D¹

Tracey Miller, Ph.D Student¹

Katherine Day, Undergraduate Research Assistant¹

¹ Climate Adaptive Design Lab, Department of Plant Science and Landscape Architecture, University of Connecticut, 1376 Storrs Road, Unit 4067, Storrs, CT

Funding for this project was provided by the United States Department of Housing and Urban Development through the Community Development Block Grant National Disaster Recovery Program, as administered by the State of Connecticut, Department of Housing. This publication does not express the views of the Department of Housing or the State of Connecticut. The views and opinions expressed are those of the authors.

Project support comes from the Connecticut Institute for Resilience and Climate Adaptation (CIRCA). CIRCA's mission is to increase the resilience and sustainability of communities vulnerable to the growing impacts of climate change on the natural, built, and human environments.

More information about CIRCA can be found at circa.uconn.edu

More information about Resilient Connecticut can be found at resilientconnecticut.uconn.edu



Table of Contents

List of Figures.....	4
List of Tables.....	4
List of Graphs.....	5
Executive Summary.....	6
1. Introduction.....	7
1.1. What is Land Surface Temperature and What is its Application?	7
2. Methods.....	8
2.1. Land-use and Land Cover (LULC) Classification.....	8
2.1.1. Local Climate Zones	8
2.1.2. LCZ Heat Sensor Network	10
2.1.3. National Land Cover Dataset (NLCD).....	11
2.2. Thermal Remote Sensing.....	14
2.2.1. Surface Emissivity.....	16
2.2.2. Normalized Difference Vegetation Index (NDVI).....	17
2.2.3. Land Surface Temperature (LST)	17
3. Results.....	20
3.1. Short-term LULC Changes: Local Climate Zones	20
3.2. Short-term in Situ Sensor Measurements for Identified LCZs in New Haven, CT.....	24
3.3. Long-term LULC Changes: National Land Cover Data Analysis	26
3.4. Long-term Land Surface Temperature Changes	28
3.5. Relationship Between LULC Changes and LST Changes Over Time	30
4. Conclusion and Recommendations.....	33
1. Glossary of Terms Used	36
2. References.....	36

List of Figures

Figure 2.1 – Local Climate Zone classification and description (Source: Stewart and Oke 2012).	9
Figure 2.2 – Sensor network deployed in New Haven in August 2020. The network composed of 20 sensors represents 10 different local climate zones (LCZs) identified in New Haven.....	10
Figure 2.3 – Comparison between the National Land Cover Dataset (NLCD) classification and the Local Climate Zone (LCZ) classification. Categories differ in the complexity offered between natural and urban landscapes.....	13
Figure 2.4 – Google Earth Engine process chain developed by Ermida et al. (2020) to retrieve Land Surface Temperature (LST) using the Landsat collection. Text in gray indicates the GEE dataset repository used to calculate the process. While the text in blue indicates the code functions that are embedded as modules. (Image source: Ermida et al. 2020).	15
Figure 2.5 - Emissivity map aligns with previous studies and indicates highest emissivity from water bodies. Variation in emissivity is present in more urbanized area.	16
Figure 2.6 – Normalized difference vegetation index (NDVI) derived in Google Earth Engine for the period between January 1, 2014 to December 31, 2019. Image is the result of the mean of all clear pixels available during the study period. Areas with low NDVI values indicate no presence or low plant health.	17
Figure 2.7 – Maximum Land Surface Temperature retrieved from January 1, 2014 to December 31, 2019. Surface temperatures during the studied period varied vastly. Ocean water was the coolest area found, while urban environments reached maximum of 141.7 degrees Fahrenheit.....	18
Figure 2.8 - Mean Land Surface Temperature retrieved from January 1, 2014 to December 31, 2019. Surface temperatures during the studied period varied vastly. Similar to maximum temperature, ocean water was the coolest surface found, while urban environments reached on average of 99.84 degrees Fahrenheit.	19
Figure 2.9 – Minimum Land Surface Temperature retrieved from January 1, 2014 to December 31, 2019. Contrary to maximum and mean images urban areas were coolest surfaces found reaching -4.43 degrees Fahrenheit. Vegetated areas displayed the highest temperatures up to 99.84 degrees Fahrenheit.	20
Figure 3.1 – Boxplot indicating overall accuracy of LCZ analysis and representation of LCZ types in New Haven county, CT (Day 2021). Overall accuracy for county was 0.64 and aligns with accuracies achieved so far in other studies in the United States, ranging between 0.77 and 0.55.....	21
Figure 3.2 - Boxplot indicating overall accuracy of LCZ analysis and representation of LCZ types in Fairfield county, CT (Miller 2021). Overall accuracy for county was 0.55 and aligns with accuracies achieved so far in other studies in the United States, ranging between 0.77 and 0.55.	22
Figure 3.3 – Final LCZ classification obtained for New Haven county displaying current conditions (Day 2021).	23
Figure 3.4 - Final LCZ classification obtained for Fairfield county displaying current conditions (Miller 2021).	24
Figure 3.5 – Psychrometric chart developed based on meteorological data retrieved from the New Haven airport. Chart indicates the number of hours in a year that are in thermal comfort, cold stress, and heat stress, and the coping strategies. The chart indicates natural ventilation as the most effective solution for hot days in New Haven.....	26
Figure 3.6 - Maximum surface temperature reached during each study period. Higher temperatures reached during 2009 to 2011 period. However, 2018 to 2020 period indicates new areas where temperatures heating has occurred.....	29
Figure 3.7 – Maximum surface temperature change between 1999 to 2020 in Fairfield and New Haven counties, CT. Map shows areas with temperature increases and decreases of up to 10 degrees Fahrenheit. Cooling areas were seen in the coast near the water, while areas with temperature increases were in western Fairfield and northeastern New Haven.....	30

List of Tables

Table 2.1 – NLCD class code correspondence table from 2001 to 2016.	12
--	----

Table 3.1 – Results obtained from in-loci sensors measuring air temperature and relative humidity, and derived heat index (August through October 2020). Mean and maximum conditions show that humidity levels play an important role in the sensation of heat.....	25
Table 3.2 - Changes in area per land cover type, indicating representation per study period and losses or gains over time.....	28

List of Graphs

Graph 3.1 - Total area of land cover type change between years ending in 2001 and 2016, ordered from most to least representative typologies.....	27
Graph 3.2 - Boxplot analysis of maximum surface variation per land cover type per study period.	31
Graph 3.3 - Comparative maximum air temperature from May through September for each study period. Source: New Haven airport meteorological station.	32
Graph 3.4 - Temperature variation estimates based on the average temperature changes between 1999 to 2016.	33

Executive Summary

Cities across the United States are challenged to make decisions on accommodating growth and promoting healthy communities in the face of climate change. In the last 30 years, extreme heat events have been the deadliest weather-related hazards in the United States. A recent report from the Yale Center for Climate Change and Health (Bozzi 2020) indicates that Connecticut residents are less adapted to heat and are more vulnerable to heat-related illnesses under extreme heat conditions than the average American. It also indicates that Connecticut has a significant proportion of the population that is more vulnerable to heat, such as those above 65 years of age, outdoor workers, and homeless people. More importantly, the report suggests that the pathway to adaptation should involve land use planning and urban design.

In order to adequately address heat vulnerability, we need to understand the interactions between land surfaces and temperature to support climate-oriented decision making. Climate data from weather stations is limited in urban areas and data on air temperature are typically captured in the shade and far from construction. To overcome these limitations, this project is grounded in previous studies in urban climatology and uses satellite imagery to understand the occurrence and intensification of urban heat islands in cities. Moreover, it seeks to generate transferable knowledge to fields such as urban planning, to support Connecticut towns in addressing and adapting to heat vulnerability.

This project combines remote sensing and localized sensor measurements to identify and understand the relationship between temperature and land cover. It focuses on Fairfield and New Haven counties in the state of Connecticut, with the possibility of expanding the analysis to the entire state. Our team used readily available satellite data (Landsat collection) and land cover classification methods and datasets to understand how changes to the landscape in these counties have impacted surface temperature in the last 20 years. In other words, this project asked the question: **what changes to the landscape have promoted or intensified the occurrence of urban heat islands?**

The findings from this study indicate that the appearance and intensification of urban heat islands in Fairfield and New Haven counties are linked to the loss of vegetation due to expansion and intensification of urbanization. More importantly, the study indicates that specific types of vegetation loss, particularly forest cover, have resulted in the biggest temperature spikes within the last 20 years. The results also indicate that though vegetation reduces the occurrence of urban heat islands, trees are far more effective in cooling surfaces for the purposes of human health and well-being.

1. Introduction

Extreme heat and cold are among the leading causes of climate vulnerability in the United States due to potential impacts on human health and well-being. Residents in Connecticut are less acclimatized to heat, which could signify a higher risk for heat-related diseases during extreme weather events. The occurrence of heat islands due to urbanization produce relatively warmer air temperatures near the ground, which make urban and sub-urban areas warmer in comparison to rural areas. This project identifies variations in surface and air temperature over time and their linkages to land cover and land uses changes. Such observations can lead to the determination of the occurrence and intensification of urban heat islands and are directly linked to land-use planning, health, and hazard mitigation, among other fields of decision-making. Therefore, the results of this project are critical to support local decision-makers in determining the thermal vulnerability of local communities in the Resilient Connecticut project.

The main objective of this study was to map and identify areas vulnerable to extreme thermal conditions and identify the contribution of the changes in land use and land cover to heat vulnerability. To do so, this project was tasked to: (1) analyze land surface temperature data, acquired from satellite images, to identify areas where heat islands are occurring; (2) understand the linkages between land surface temperature (LST) changes and land use and land cover (LULC) changes, to interpret the relationships between thermal variation and urbanization over the past 5- and 20-years; and (3) compare the urban heat island intensity on human health and well-being by using air temperature and Landsat land surface temperature.

1.1. What is Land Surface Temperature and What is its Application?

In simple terms, land surface temperature (LST) is the temperature that any given surface of the Earth would feel to the human touch. It varies depending on the surface, as each material differs on how it absorbs or conducts heat. Therefore, LST is not the same as air temperature, which we are accustomed to seeing in a weather report. Yet it is a useful and established proxy to understanding the occurrence of urban heat islands (UHI) (Voogt and Oke 2003, Weng and Quattrochi 2006). Though LST differs from air temperature, there is a relationship between them. For instance, imagine hovering your hand over a hot pan. As the surface of the pan heats up, so does the air that surrounds it. Therefore, as you hover your hand over the surface you feel the effects of the heat emitted from the pan in the air. So why not simply measure the air temperature? It is important to note that meteorological data is not widely available and weather stations are typically not sited in urban locations. Also, stations typically collect data in the shade and do not offer long-term information on temperature variations in different land cover types. Hence the use of thermal satellite data, which has been available since the early 1980s when NASA launched Landsat satellite missions 4 and 5.

Urban heat islands (UHI) in simple terms are the effect of changes in land cover which alter surface temperature and ultimately change the transference of heat to the air. Past studies have indicated that UHIs are more evident within urban environments with satellite data and are strongly related to land cover (Aniello et al. 1995, Dousset and Gourmelon 2003). Moreover, studies in heat vulnerability have indicated that LST can be a strong predictor of heat related mortality during extreme heat events (Johnson and Wilson 2009, Johnson, Wilson and Luber 2009, Dousset et al. 2011).

So far, the use of thermal satellite images has produced better understandings of the relationships between urban surfaces, specifically LULC, to temperature changes in urban environments (Weng, Lu and Schubring 2004, Yuan and Bauer 2007, Buyantuyev and Wu 2010, Zhou, Huang and Cadenasso 2011, Zhou et al. 2014, Fu and Weng 2016). Yet, as described by Zhou et al. (2014), vegetation abundance and impervious cover are consistently identified as the most important determinants of LST increases. However, the simple division between 'rural' (vegetated) and 'urban' (impervious surface area) do not account for the complexities of the land covers observed in our environments, as discussed by Stewart and Oke (2012). With that in mind, this study goes further and uses LST and different land cover classifications to try to better understand what types of land cover and land-uses result in higher or lower temperature variation. This information can support decision-making that fosters conservation of critical landscapes and supports the restoration and promotion of native greening within the state of Connecticut.

2. Methods

2.1. Land-use and Land Cover (LULC) Classification

2.1.1. Local Climate Zones

In the first phase of the project the team applied the local climate zones (LCZ) classification (Stewart and Oke 2012, Stewart, Oke and Krayenhoff 2014) to understand the current land cover types and how they relate to surface temperature variations (Figure 2.1). The LST classification is informed by fields such as architecture and land use planning to understand how density, impervious cover, and presence of vegetation affect local climate. This is not a readily available classification; however, it can inform decision-making, particularly for towns that are moving from Euclidean based land-use planning to form based planning codes. However, LST is mostly focused on urban environments and does not classify natural environments with the same level of complexity as it does developed landscapes.

The team relied on the World Urban Database and Access Portal Tools (WUDAPT) methodology developed to systematically apply the LST classification (Ching et al 2018). WUDAPT is a machine learning method that relies on Landsat imagery to classify existing land cover type (Bechtel et al 2019). When the project began the team followed the workflow using Google Earth Pro and SAGA GIS, as proposed by Bechtel et al 2019. All products produced were submitted through the WUDAPT portal for quality assessment. However, in 2021 WUDAPT developed the LCZ generator led by a team of researchers in Ruhr University Bochum and the team no longer relied on the previous workflow, and followed new protocols established by Demuzere, Kittner, and Bechtel (2021). The data developed for both Fairfield (Miller 2021) and New Haven (Day 2021) counties was submitted separately in the LCZ generator and are readily available in the LCZ Generator portal (<https://lcz-generator.rub.de/submissions>).

It is important to point out that both Fairfield and New Haven counties are not densely urbanized areas when compared to other regions in the U.S. and abroad. Therefore, not all LCZ types were identified in the study area, as presented in the results. For example, LCZ type 1 – Compact high-rise is not present in either of the studied counties, nor was LCZ type 4 – Open high-rise. Other types were also less prevalent and limited the machine learning approach due to the specifications needed by the workflow to indicate at least 5 sample areas with a minimum of 1km² (247 acres).

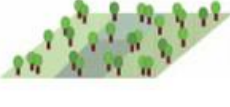
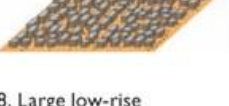
Built types	Definition	Land cover types	Definition
 <p>1. Compact high-rise</p>	Dense mix of tall buildings to tens of stories. Few or no trees. Land cover mostly paved. Concrete, steel, stone, and glass construction materials.	 <p>A. Dense trees</p>	Heavily wooded landscape of deciduous and/or evergreen trees. Land cover mostly pervious (low plants). Zone function is natural forest, tree cultivation, or urban park.
 <p>2. Compact midrise</p>	Dense mix of midrise buildings (3–9 stories). Few or no trees. Land cover mostly paved. Stone, brick, tile, and concrete construction materials.	 <p>B. Scattered trees</p>	Lightly wooded landscape of deciduous and/or evergreen trees. Land cover mostly pervious (low plants). Zone function is natural forest, tree cultivation, or urban park.
 <p>3. Compact low-rise</p>	Dense mix of low-rise buildings (1–3 stories). Few or no trees. Land cover mostly paved. Stone, brick, tile, and concrete construction materials.	 <p>C. Bush, scrub</p>	Open arrangement of bushes, shrubs, and short, woody trees. Land cover mostly pervious (bare soil or sand). Zone function is natural scrubland or agriculture.
 <p>4. Open high-rise</p>	Open arrangement of tall buildings to tens of stories. Abundance of pervious land cover (low plants, scattered trees). Concrete, steel, stone, and glass construction materials.	 <p>D. Low plants</p>	Featureless landscape of grass or herbaceous plants/crops. Few or no trees. Zone function is natural grassland, agriculture, or urban park.
 <p>5. Open midrise</p>	Open arrangement of midrise buildings (3–9 stories). Abundance of pervious land cover (low plants, scattered trees). Concrete, steel, stone, and glass construction materials.	 <p>E. Bare rock or paved</p>	Featureless landscape of rock or paved cover. Few or no trees or plants. Zone function is natural desert (rock) or urban transportation.
 <p>6. Open low-rise</p>	Open arrangement of low-rise buildings (1–3 stories). Abundance of pervious land cover (low plants, scattered trees). Wood, brick, stone, tile, and concrete construction materials.	 <p>F. Bare soil or sand</p>	Featureless landscape of soil or sand cover. Few or no trees or plants. Zone function is natural desert or agriculture.
 <p>7. Lightweight low-rise</p>	Dense mix of single-story buildings. Few or no trees. Land cover mostly hard-packed. Lightweight construction materials (e.g., wood, thatch, corrugated metal).	 <p>G. Water</p>	Large, open water bodies such as seas and lakes, or small bodies such as rivers, reservoirs, and lagoons.
 <p>8. Large low-rise</p>	Open arrangement of large low-rise buildings (1–3 stories). Few or no trees. Land cover mostly paved. Steel, concrete, metal, and stone construction materials.	VARIABLE LAND COVER PROPERTIES	
 <p>9. Sparsely built</p>	Sparse arrangement of small or medium-sized buildings in a natural setting. Abundance of pervious land cover (low plants, scattered trees).	<p><i>b. bare trees</i></p>	Leafless deciduous trees (e.g., winter). Increased sky view factor. Reduced albedo.
 <p>10. Heavy industry</p>	Low-rise and midrise industrial structures (towers, tanks, stacks). Few or no trees. Land cover mostly paved or hard-packed. Metal, steel, and concrete construction materials.	<p><i>s. snow cover</i></p>	Snow cover >10 cm in depth. Low admittance. High albedo.
		<p><i>d. dry ground</i></p>	Parched soil. Low admittance. Large Bowen ratio. Increased albedo.
		<p><i>w. wet ground</i></p>	Waterlogged soil. High admittance. Small Bowen ratio. Reduced albedo.
			Variable or ephemeral land cover properties that change significantly with synoptic weather patterns, agricultural practices, and/or seasonal cycles.

Figure 2.1 – Local Climate Zone classification and description (Source: Stewart and Oke 2012).

The first portion of analysis using the old WUDAPT methodology allowed our team to analyze 10 sets of Landsat 8 Tier 1 images, with cloud cover below 10%, for the years of 2019 (July, August, September, and November 2019, and February 2020) and 2015 (January, March, April, August, and October). The images used in the machine learning process, proposed by WUDAPT, used samples from various seasons to ensure that we were classifying the climate zones correctly. During summer and spring, the lush tree canopy cover often obscures development in satellite images. By using multiple seasons, we were able to identify many areas that were initially classified as forested but were in fact sparsely built. All images were clipped to a region of interest that encompasses a 20km buffer from the outer edges of each county's boundary, including surrounding towns. This approach follows the methodology outlined by WUDAPT and allowed a better assessment of the diversity of land cover types that currently exist within the region.

2.1.2. LCZ Heat Sensor Network

As a starting point for the LCZ classification the team established the city of New Haven as a prototype to streamline the land cover methodology for the entire study area. This approach enabled the team to develop a classification library that depicts the LCZ classification as seen in the region (Appendix 1). Moreover, the initial classification of New Haven allowed for the deployment of a heat and humidity sensor network to retrieve data based on different LCZ classification types identified in the city. The network is composed of 20 sensors deployed in New Haven (Figure 2.2) and the analysis period presented in this report corresponds to consistent data retrieved between August 2020 and October 2020. Some sensors malfunction after the analysis period and were substituted. This allowed the team to evaluate the distribution and adequate representation of the LCZ types identified in the region. Some of the sensors were relocated to better represent the LCZ classes and a new round of measurements began in the summer of 2021.

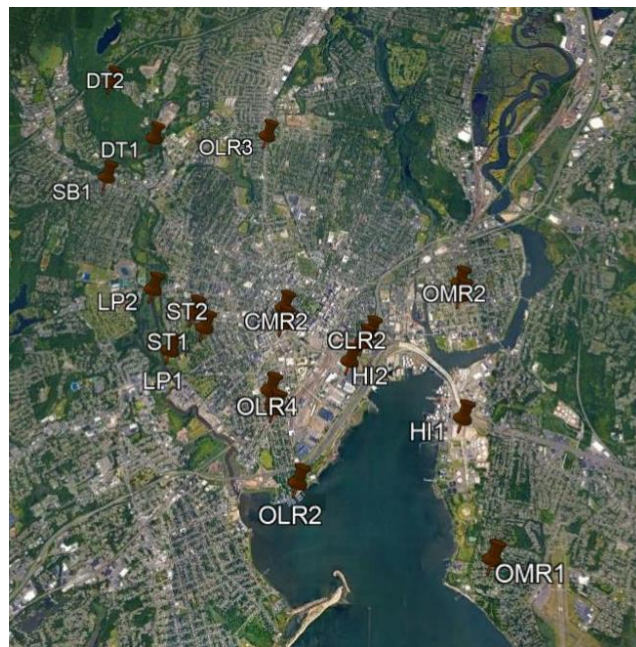


Figure 2.2 – Sensor network deployed in New Haven in August 2020. The network composed of 20 sensors represents 10 different local climate zones (LCZs) identified in New Haven.

The data retrieved from the sensors was extracted in tabular form. The analysis focused on mean and maximum temperatures reached during the studied period and evaluated the resulting heat index. The heat index is a common metric used by the CDC and National Weather Service (NWS) to determine the sensation of heat and its potential health risks. The heat index is a useful metrics to understand the impacts of heat in the human body. For instance, at high temperature and high humidity the human body struggles to perspire, therefore, it is unable to cool down.

To assess the heat index for the readings gathered the team applied a series of equations depending upon the readings obtained. If heat index results were below 80 °F the simplified heat index equation was applied (Equation 1). However, for heat index above 80 °F, temperature between 80 °F and 87 °F, and relative humidity greater than 85% the Rothfusz equation (Equation 2) was applied followed by an adjustment added to the resulting heat index (Equation 3) (Rothfusz 1990).

$$HI = 0.5 * \{T + 61.0 + [(T-68.0)*1.2] + (RH*0.094)\}$$

Where:

HI= Heat Index

T= Temperature (degrees Fahrenheit)

RH= Relative Humidity (percentage)

Equation 1

$$HI = -42.379 + 2.04901523*T + 10.14333127*RH - .22475541*T*RH - .00683783*T*T - .05481717*RH*RH + .00122874*T*T*RH + .00085282*T*RH*RH - .00000199*T*T*RH*RH$$

Equation 2

$$ADJUSTMENT = [(RH-85)/10] * [(87-T)/5]$$

Equation 3

2.1.3. National Land Cover Dataset (NLCD)

The National Land Cover Dataset (NLCD) is a readily available land cover classification developed by the U.S. Geological Survey (USGS) in cooperation with the Multi-Resolution Land Characteristics Consortium (MRLC). This dataset is derived from Landsat satellite images and land cover products result from three-year analysis periods for the contiguous U.S. and Puerto Rico. This study used land cover products for 2001 (based on years 1999 to 2001), 2006 (based on years 2004 to 2006), 2011 (based on years 2009-2011), and 2016 (based on years 2014-2016). The land cover products were used to develop change analysis retrieved using two approaches: (a) the generation of a land cover change map containing coded values for observed land cover (Table 2.1); and (b) the generation of a land cover change matrix, indicating the areal coverage of changes for Fairfield and New Haven counties. These representations were then used to statistically interpret how land cover change might contribute to increases in surface temperature.

Table 2.1 – NLCD class code correspondence table from 2001 to 2016.

Description	NLCD class code
Open water	11
Perennial ice, snow	12
Urban, recreational grasses	21
Low intensity residential	22
High intensity residential	23
Commercial, industrial, roads	24
Bare rock, sand	31
Quarry, strip mine, gravel pit	31
Transitional barren	31
Deciduous forest	41
Evergreen forest	42
Mixed forest	43
Shrubland	52
Orchards, vineyards, other	82
Grasslands, herbaceous	71

LCZ and NLCD are complementary datasets that enable the understanding of the diversity of both vegetated and developed environments. Contrary to the LCZ classification, NLCD offers a wider variety of classifications for natural landscapes versus urban landscapes. It divides urban environments in only four categories, while LCZ provides ten distinct categories (Figure 2.3 and Appendix 2). Yet, as previously mentioned, NLCD is a long standing and readily available dataset that would support immediate action for decision-makers, whereas LCZ is not widely used. Furthermore, the WUDAPT methodology applied to obtain the LCZ classification is still evolving. The machine learning approach seems to render higher accuracy in dense urban areas and seems to be less refined to interpret suburban areas with less urban density and a higher diversity of vegetation types. Both Fairfield and New Haven Counties did not present categories such as compact high-rise and compact mid-rise that are present in dense urban areas. While open mid-rise had a limited amount of sampling available, which limit the accuracy of the classification. Most importantly, the use of both datasets aids in overcoming the LCZ limitations. It also enables the understanding of what specific types of vegetation are loss versus what specific types of development is gained. This combination could be the key to outlining a path to heat response planning as a component of city planning and conservation.

NLCD: National Landcover Dataset

LCZ: Local Climate Zone

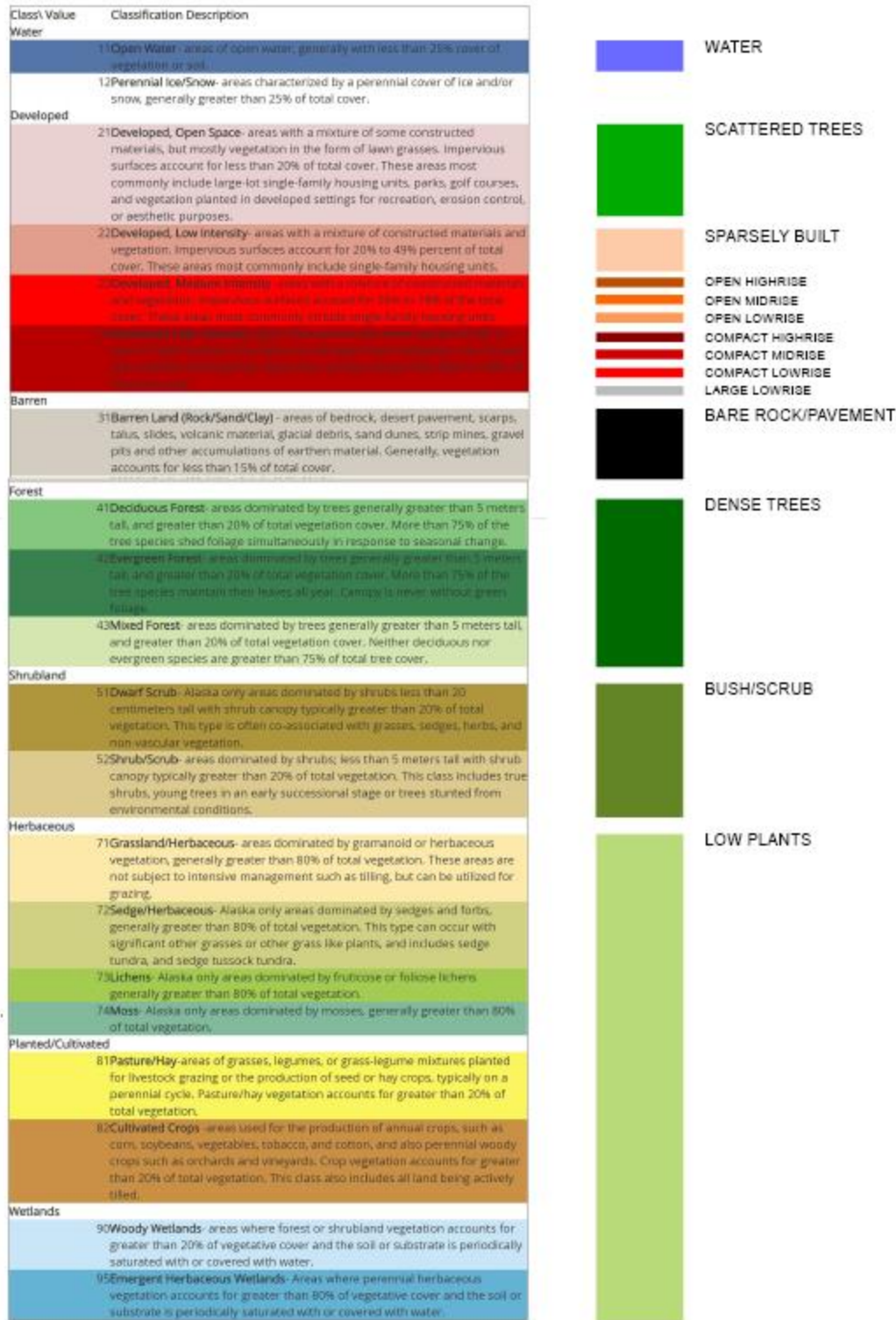


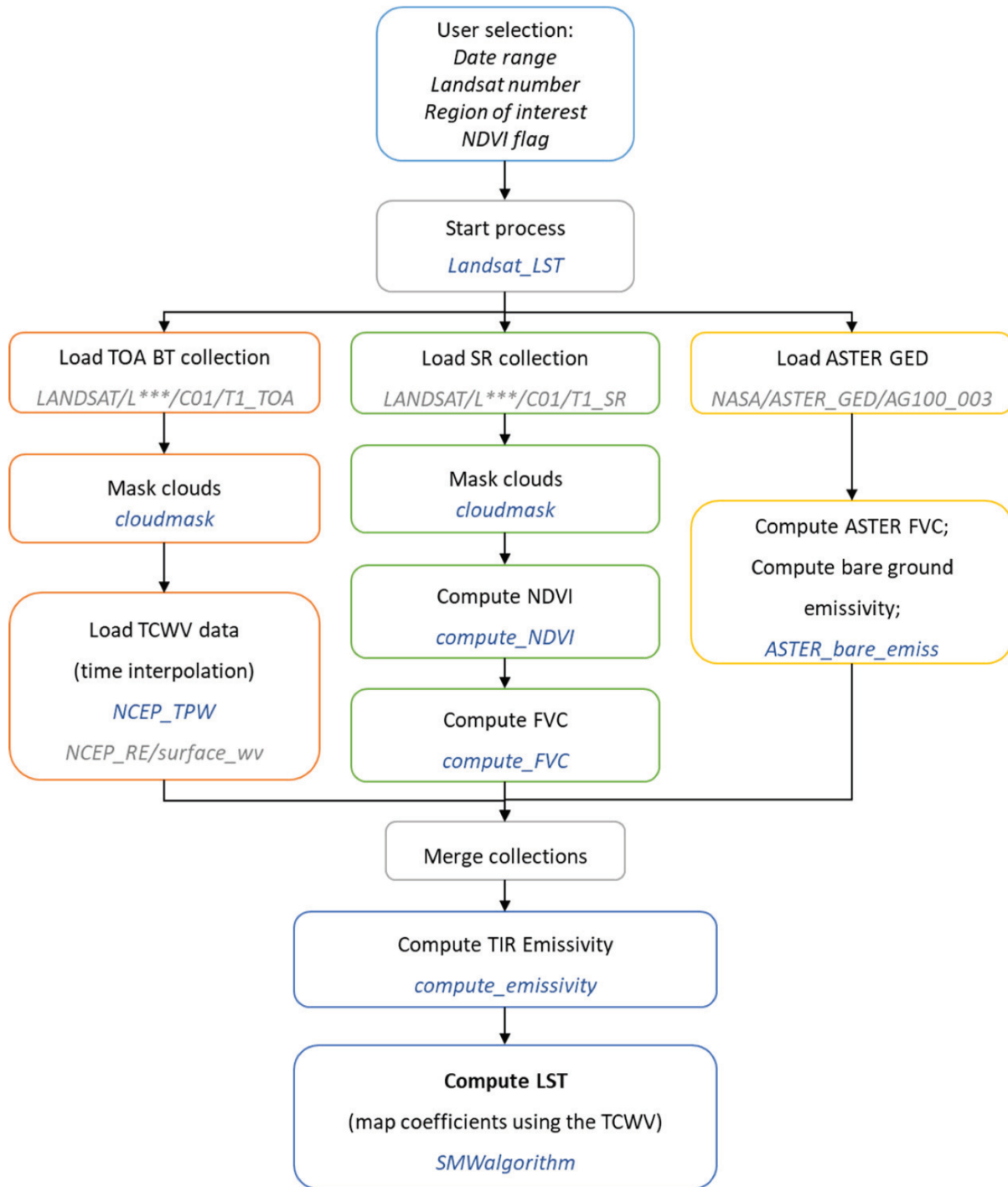
Figure 2.3 – Comparison between the National Land Cover Dataset (NLCD) classification and the Local Climate Zone (LCZ) classification. Categories differ in the complexity offered between natural and urban landscapes.

2.2. Thermal Remote Sensing

The methodology applied for thermal remote sensing in this project is based on methods outlined by Ermida et.al. (2020), and its resulting GEE code repository that allowed us to compute LST and supplementary data from Landsat collections. This approach for urban heat island analysis was presented by NASA's Earth Science Applied Sciences program and is integrated in the Applied Remote Sensing Training program (ARSET, 2020). Moreover, the methodology proposed by Ermida et al. (2020) is calibrated and validated with in-situ LST measurements. The choice of a readily available methodology for retrieving satellite remote sensing for urban heat islands allows for the replicability of this study to the entire state of Connecticut, and ensures that the data derived is comparable to other ongoing urban heat island analysis developed at the regional and national scale.

The free and open sourced code used in this study follows a processing chain in GEE to derive LST outputs (Figure 2.4). The process chain retrieves data from different datasets available in the GEE database repository. The chain first derives the input data needed to compute LST. Top of atmosphere (TOA) brightness temperature is acquired using Landsat's thermal infrared (TIR) bands. Atmospheric contributions to the TIR observations are accounted for using Total Column Water Vapor (TCWV) values retrieved from the NCEP/NCAR reanalysis data. Surface emissivity and NDVI are derived as part of the input data needed to derive the LST. Cloud masking is also applied throughout the chain process, as seen in Figure 1. We derived data from the Landsat 5 and 8 satellites Tier 1 collection, given the timeframe of analysis (1999-2019), which is fully implemented in GEE. Adaptions made to the script included changes to the geographic location, centered on Fairfield and New Haven counties, and date and range parameters.

A total of 89 images were analyzed for the 5-year study period (1 January 2015 to 31 December 2019), while 238 images were used for the 20-year analysis period. Due to the Landsat Acquisition plan, images retrieved from both Landsat 5 and Landsat 8 were collected every 16 days and retrieval time varied between approximately 3:15 p.m. for Landsat 5 and approximately 3:30 p.m. for Landsat 8 (+/- 15 minutes, mean local time).



Module GEE dataset

Figure 2.4 – Google Earth Engine process chain developed by Ermida et al. (2020) to retrieve Land Surface Temperature (LST) using the Landsat collection. Text in gray indicates the GEE dataset repository used to calculate the process. While the text in blue indicates the code functions that are embedded as modules. (Image source: Ermida et al. 2020).

2.2.1. Surface Emissivity

As mentioned previously, the surface emissivity data derived in this project is a required input for the LST retrieval algorithm used in GEE. This data is derived from the ASTER GEDv3 dataset developed by Hulley et al. (2015). This dataset corresponds to the average of all TIR retrievals (5 bands) over an eight-year period. Accuracy of the emissivity data was of approximately 0.01, with spatial resolution of 100m (Ermida et al. 2020). This process needs to account for vegetation density which is accomplished through the incorporation of fraction of vegetation cover (FVC) (Malakar et al., 2018; Parastatidis et al., 2017). Therefore, the emissivity outputs for this phase of the project was corrected using FVC, derived from NDVI inputs. The GEE code provided by Ermida et al. (2020), follows the relationship proposed by Carlson and Ripley (1997):

$$FVC = \left(\frac{NDVI - NDVI_{bare}}{NDVI_{veg} - NDVI_{bare}} \right)^2$$

Equation 4

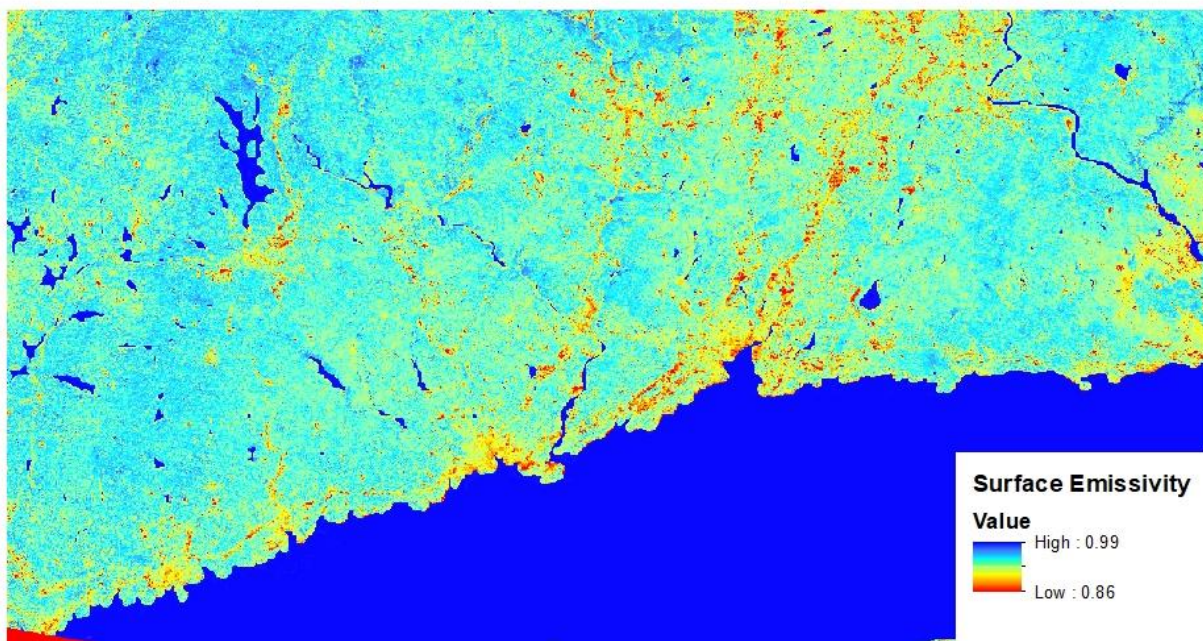


Figure 2.5 - Emissivity map aligns with previous studies and indicates highest emissivity from water bodies. Variation in emissivity is present in more urbanized area.

As seen in Figure 2.5, the resulting emissivity map confirms findings from previous studies. The variation in material composition and ranging albedo in urbanized areas leaves a clear signature. The results obtained align with findings from Mitraka et al. (2011), which show that darker surface materials have average emissivity equal to 0.979, while high-albedo construction materials have mean emissivity value equal to 0.94. Vegetation emissivity is estimated on average to equal 0.987, while soil types have a mean emissivity of 0.973.

2.2.2. Normalized Difference Vegetation Index (NDVI)

NDVI is a needed input to generate the FVC, and accounts for variations in annual and inter-annual vegetation density, averaged out in the TIR retrieval process of the ASTER GEDv3 dataset. Following the GEE process chain, NDVI is retrieved using both Landsat derived NDVI and mean ASTER GEDv3 NDVI (Malakar et al., 2018). The code was altered to generate the mean NDVI for the study period (January 1, 2014 to December 31, 2019).

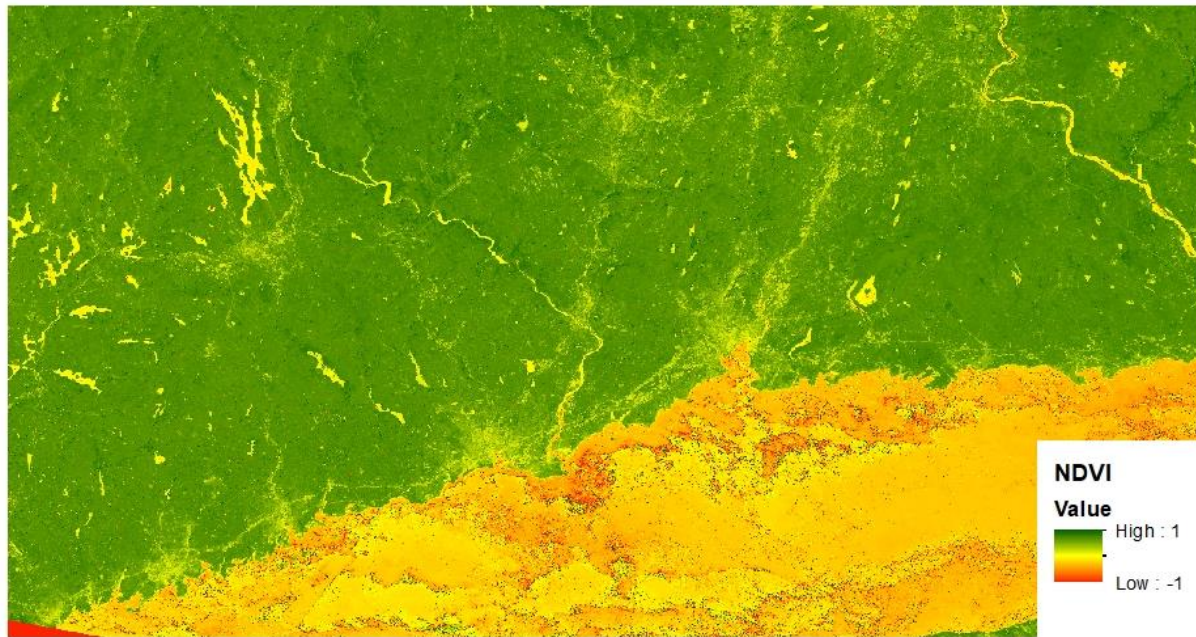


Figure 2.6 – Normalized difference vegetation index (NDVI) derived in Google Earth Engine for the period between January 1, 2014 to December 31, 2019. Image is the result of the mean of all clear pixels available during the study period. Areas with low NDVI values indicate no presence or low plant health.

The NDVI results (Figure 2.6) also aligned with expected findings, showing clear signatures of no vegetation and reduced health in and around developed areas. Major expressways have clear signatures on the landscape. Water bodies are also clearly depicted given the inexistence of vegetation in these surfaces.

2.2.3. Land Surface Temperature (LST)

LST was retrieved by the code using the statistical mono-window (SMW) algorithm from the Climate Monitoring Satellite Application Facility (CM-SAF). This method uses simple linear regression to linearize the radiative transfer equation and maintain the dependence on surface emissivity (Equation 5). In other words, it examines the relationship between TOA brightness temperatures in each TIR channel and LST.

$$LST = A_i \frac{Tb}{\varepsilon} + B_i \frac{1}{\varepsilon} + C_i$$

Equation 5

where T_b is the TOA brightness temperature in each TIR channel, ϵ is the surface emissivity for the channel, and A_i , B_i , and C_i are the result of linear regressions of radiative transfer simulations for 10 classes of TCWV ($i=1$ through 10).

The code was altered to derive three (3) LST outputs that could summarize the amplitude of land surface temperature. The original code sought to represent the first clear image for a given time range. For this study, the code was altered to compute the mean, maximum, or minimum temperatures reached. Additionally, the time range was broadened from days to years.

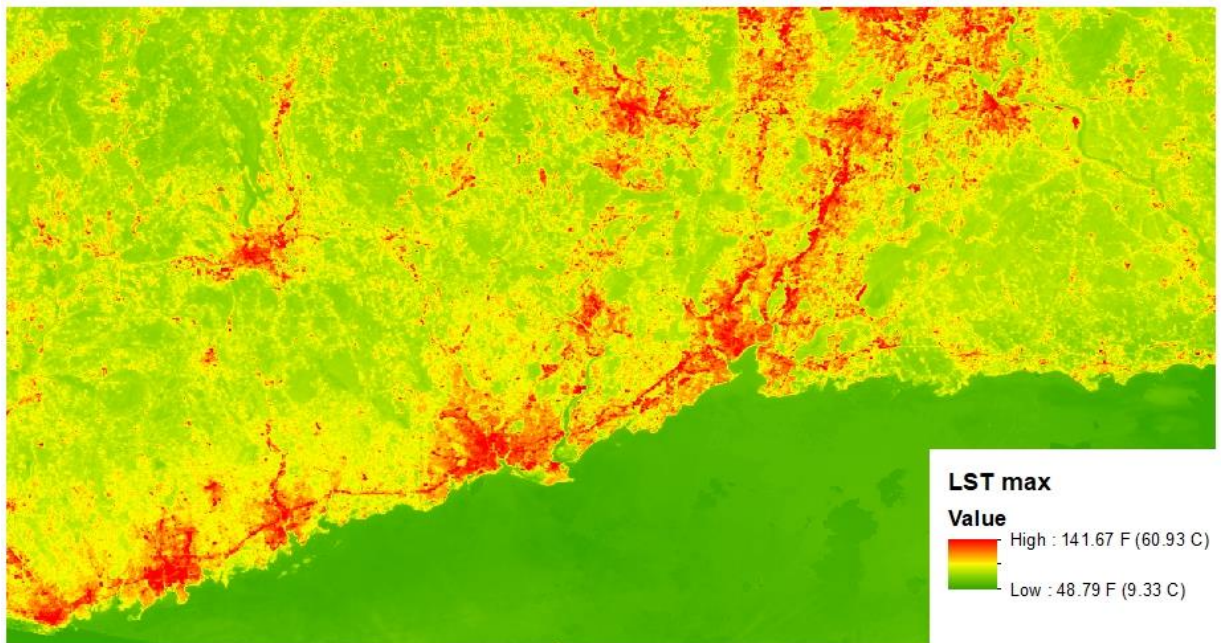


Figure 2.7 – Maximum Land Surface Temperature retrieved from January 1, 2014 to December 31, 2019. Surface temperatures during the studied period varied vastly. Ocean water was the coolest area found, while urban environments reached maximum of 141.7 degrees Fahrenheit.

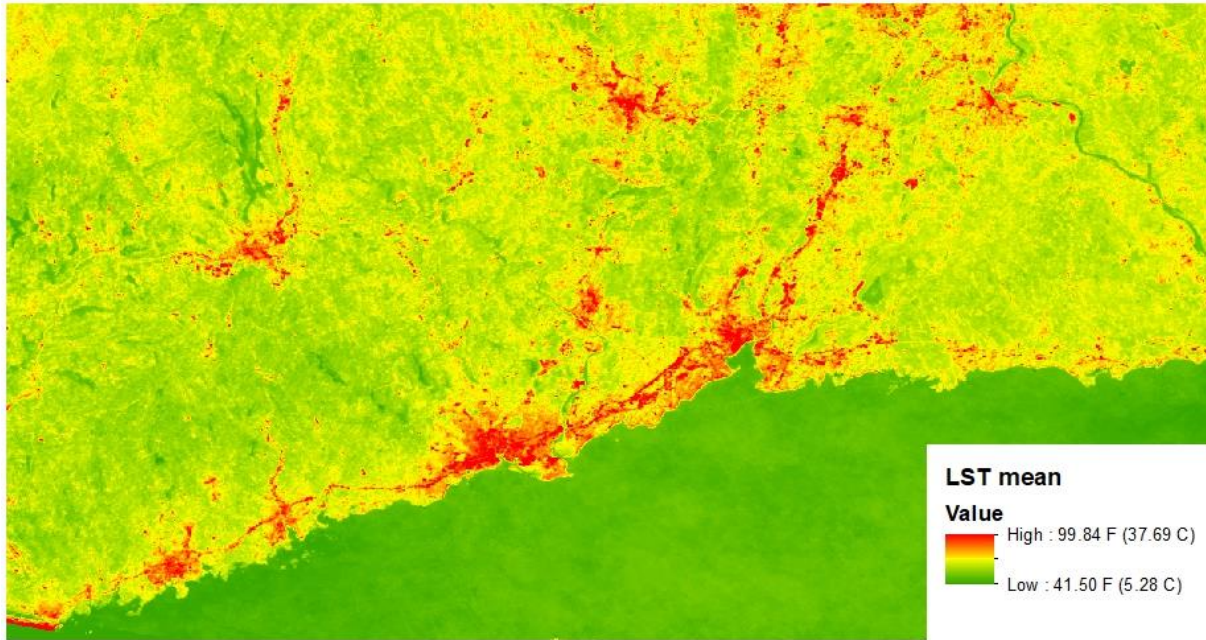


Figure 2.8 - Mean Land Surface Temperature retrieved from January 1, 2014 to December 31, 2019. Surface temperatures during the studied period varied vastly. Similar to maximum temperature, ocean water was the coolest surface found, while urban environments reached on average of 99.84 degrees Fahrenheit.

Figure 2.7 and 2.8 depict maximum and mean LST analysis. In both images urban centers are highlighted and show a clear distinction between the cool surrounding water bodies and vegetated environments and the warm thermal signature experienced in urban areas. However, in contrast, Figure 2.9 shows how the urban environment during winter months can become colder than its surrounding environments. The combined understanding of the three images retrieved in this study indicate the thermal variation of these environments. Moreover, the contrasting low temperatures correspond to snow accumulation and potential impacts of impervious covers under maximum and minimum thermal conditions.

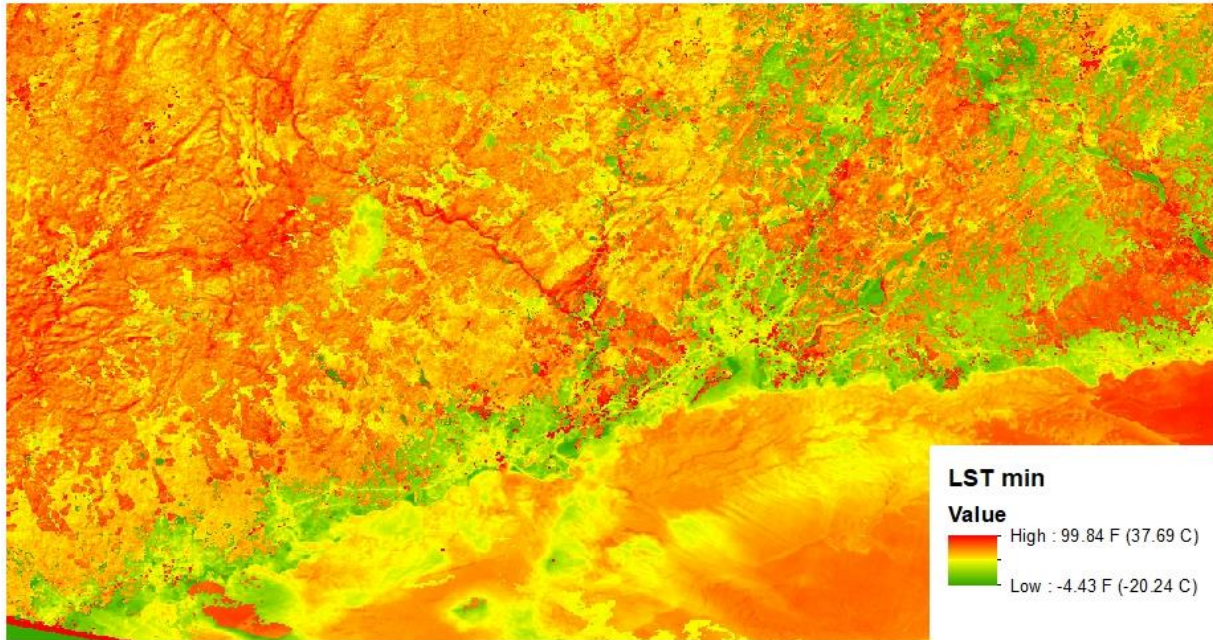


Figure 2.9 – Minimum Land Surface Temperature retrieved from January 1, 2014 to December 31, 2019. Contrary to maximum and mean images urban areas were coolest surfaces found reaching -4.43 degrees Fahrenheit. Vegetated areas displayed the highest temperatures up to 99.84 degrees Fahrenheit.

3. Results

3.1. Short-term LULC Changes: Local Climate Zones

The first iteration of this phase of analysis showed some discrepancies with maps indicating a pessimistic classification that found a higher level of urbanization in the analyzed region or an overly optimistic classification that showed a much higher level of forested cover. This iteration indicated predominance of open low-rise and large low-rise in the coastal shoreline towns, and higher presence of sparsely built or dense forest type land covers in the interior towns. As illustrated in Appendix 2, which shows the iterations of classification for the 5-year study period for both counties. The second iteration was better calibrated yet there were conflicts between the edge towns of the counties, which indicated variations in interpretation from the machine learning system. To resolve this, further training zones were created and a revision on the parameters were proposed to reduce the conflicts in classification.

The third iteration of analysis indicates that category indicated that variations seen in previous iterations were related to pervious and impervious percentage parameters that seemed to differ from those established in the scientific literature. Analysis of plans of conservation and impervious dataset indicated that rural residential areas in the region are dominated by large lots that go beyond the 60% to 80% pervious threshold proposed by the LCZ classification (Stewart and Oke 2012). To better interpret these perceived errors, the team incorporated the use of GIS-based impervious and pervious percentages to aid in the calibration of training areas applied in the machine learning process. This enabled the adjustment of LCZ training areas to a higher percentage of pervious cover (97%) to better represent the existing land cover types based on form and use. A total of four iterations were made of the LCZ classifications for each county, using the World Urban Database and Access Portal Tools (WUDAPT) methodology. The final iteration was then submitted to the LCZ Classification portal for accuracy evaluation (Figures 3.1 and 3.2) and publishing (Figure 3.3 and 3.4).

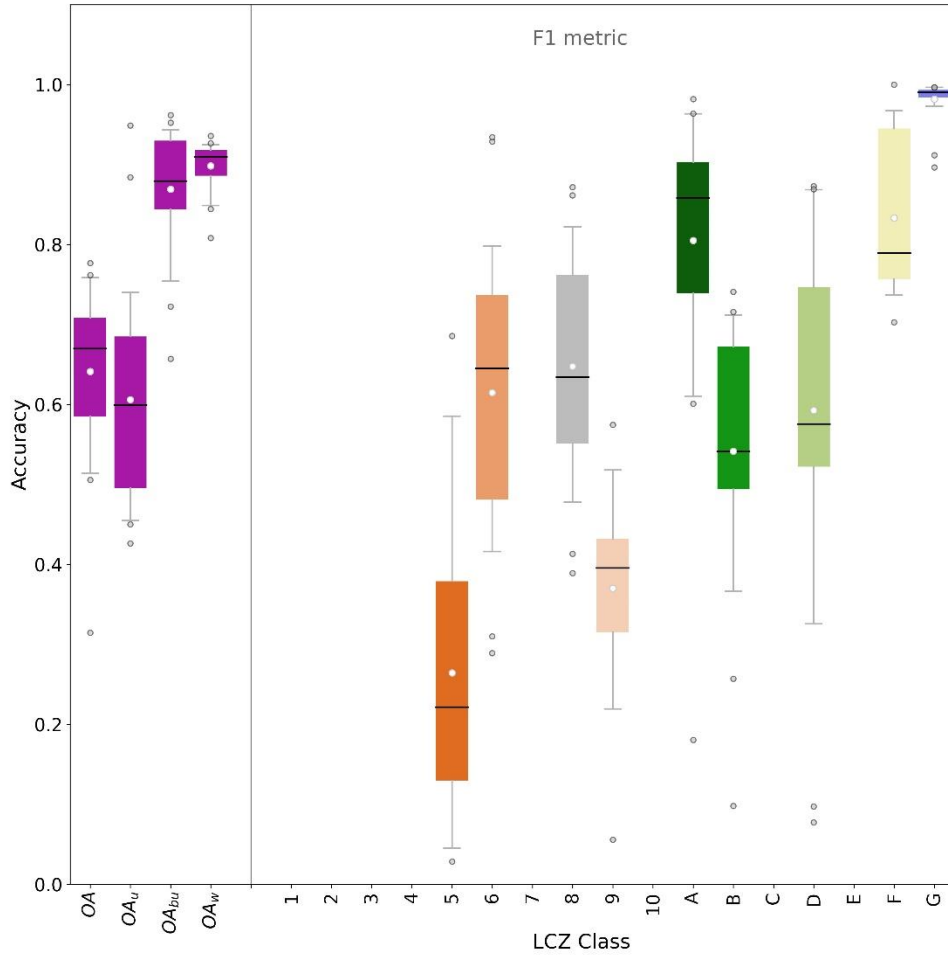


Figure 3.1 – Boxplot indicating overall accuracy of LCZ analysis and representation of LCZ types in New Haven county, CT (Day 2021). Overall accuracy for county was 0.64 and aligns with accuracies achieved so far in other studies in the United States, ranging between 0.77 and 0.55.

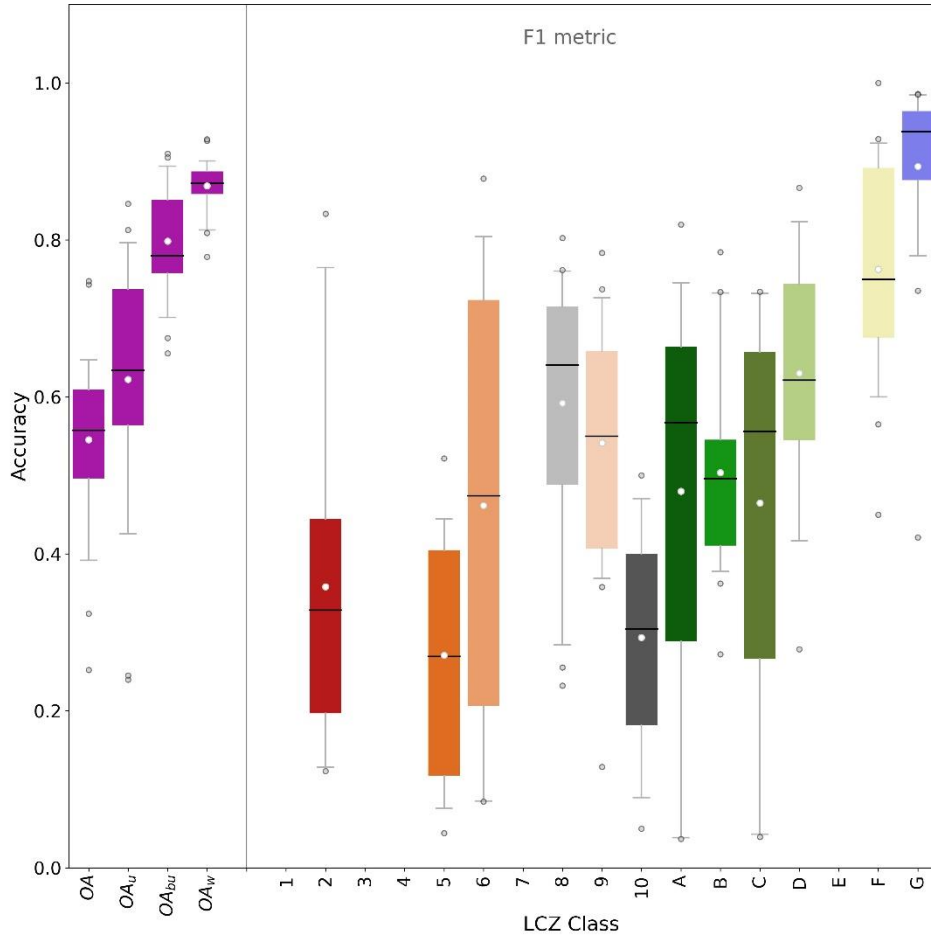


Figure 3.2 - Boxplot indicating overall accuracy of LCZ analysis and representation of LCZ types in Fairfield county, CT (Miller 2021). Overall accuracy for county was 0.55 and aligns with accuracies achieved so far in other studies in the United States, ranging between 0.77 and 0.55.

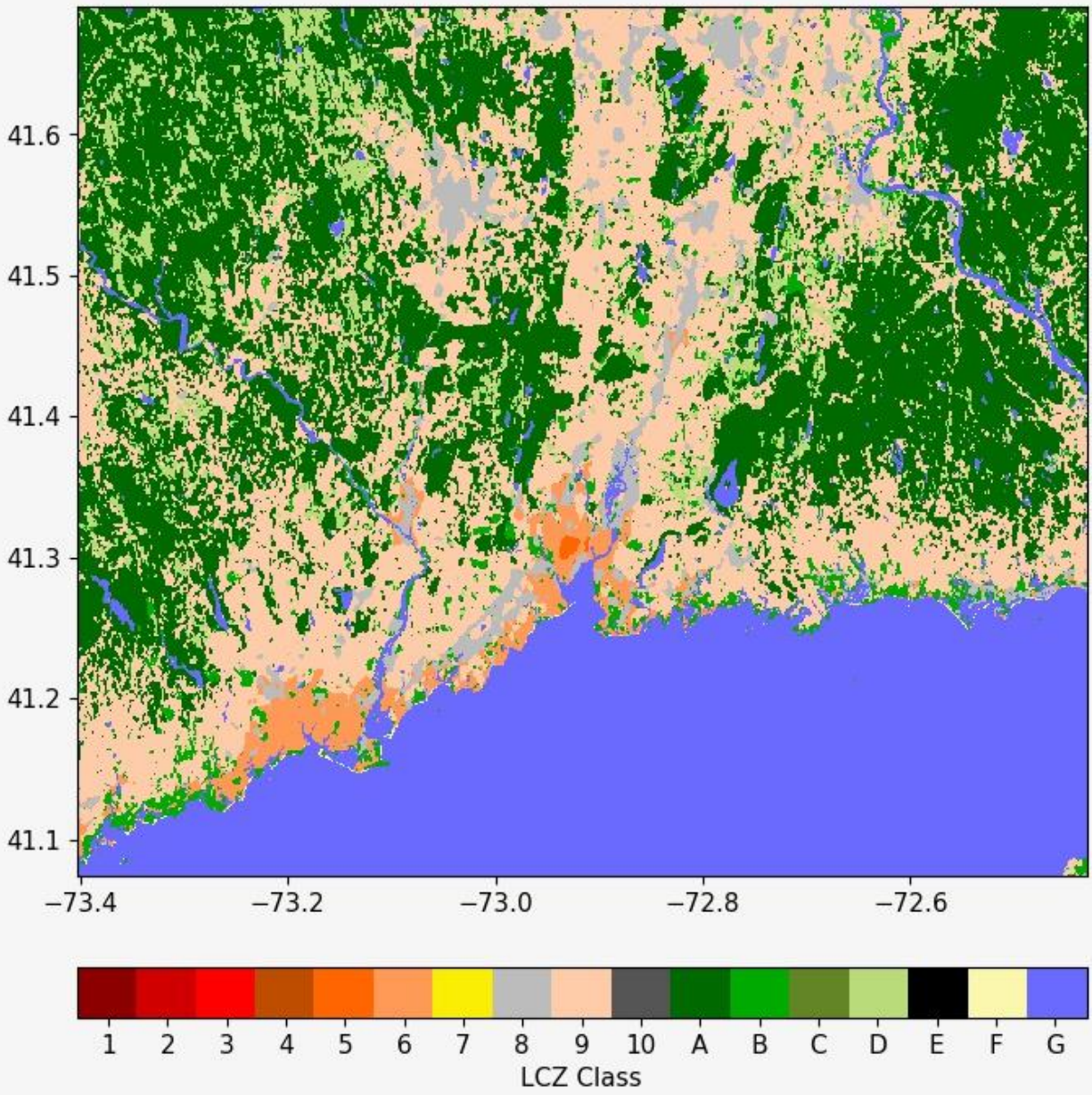


Figure 3.3 – Final LCZ classification obtained for New Haven county displaying current conditions (Day 2021).

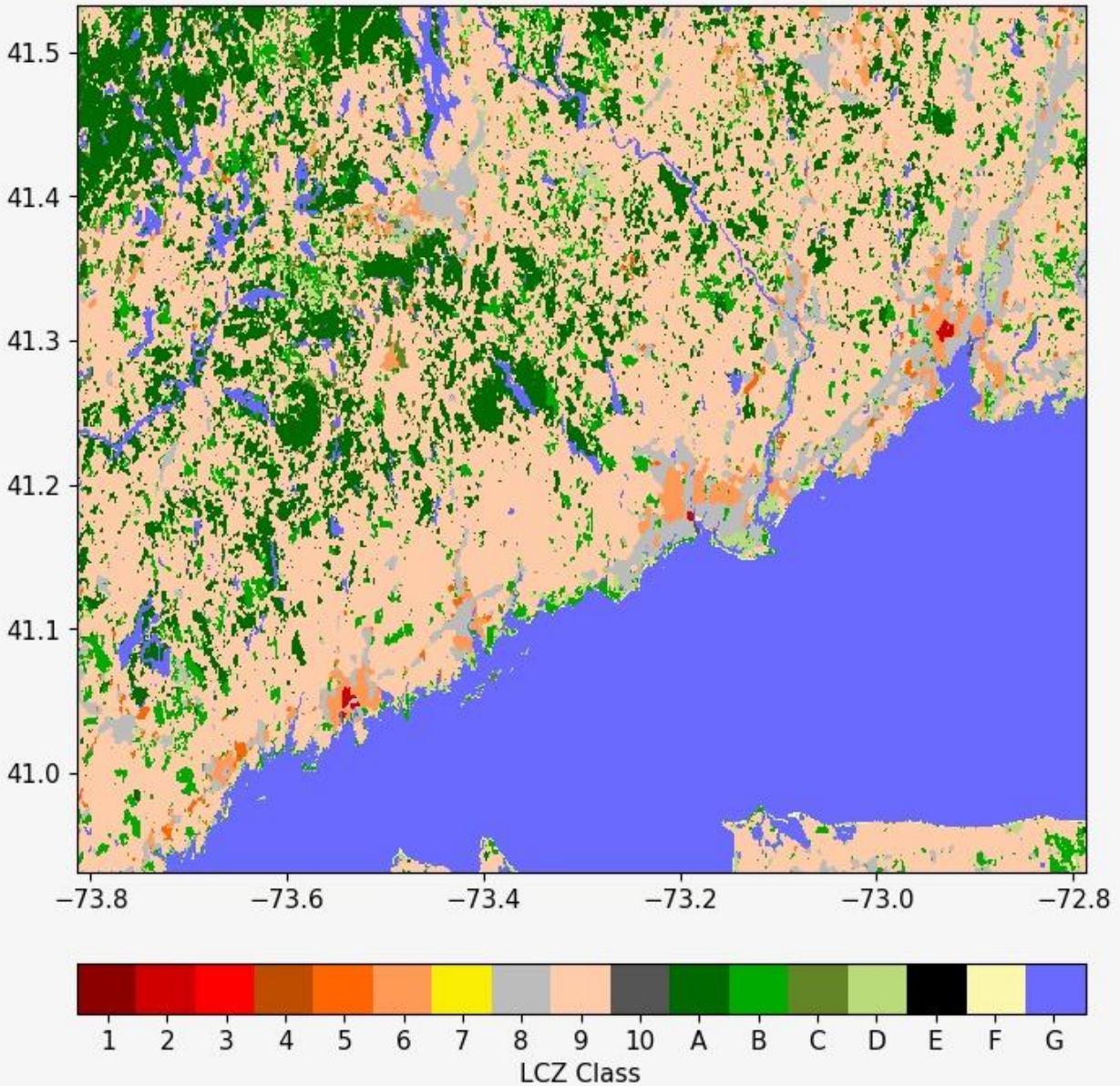


Figure 3.4 - Final LCZ classification obtained for Fairfield county displaying current conditions (Miller 2021).

3.2. Short-term in Situ Sensor Measurements for Identified LCZs in New Haven, CT

The sensor network that resulted from the prototype classification developed in New Haven shows the variations in air temperature and relative humidity across the different typologies identified (Table 3.1). The readings from the sensors allowed us to calculate the heat index to interpret the sensation of heat in each of the studied environments. The results presented in Table 3.1 indicate that humidity is an important factor in heat vulnerability, not seen in the remote sensing analysis. Therefore, locations where humidity is high resulted in a higher sensation of heat. Mean temperature readings averaged between 71.66- and 74.42-degrees Fahrenheit in vegetated areas, while urban settings ranged between 73.76- and 76.11-degrees Fahrenheit. Relative humidity was lower in developed landscapes compared

to vegetated ones. This was not surprising as plants tend to contribute to increase humidity. Overall, areas with low rise development and low plants had higher heat index under mean temperature conditions. Under maximum temperature conditions readings showed larger variation in heat index results. Relative humidity was mostly between upper 90 to 100 percent, except for site OLR2 which reached a maximum of 73.03%. Maximum temperatures varied between 91.94- and 97.81-degrees Fahrenheit in developed landscapes, while vegetated locations varied between 88.71- and 96.38-degrees Fahrenheit.

The combination of high humidity and high temperature indicated that the highest heat indexes were situated in the scattered tree areas and the heavy industrial sites. Yet, the highest results seem surprising given the presence of trees. Equally surprising were the low results obtained for the compact mid-rise sites, which were only 1-degree Fahrenheit cooler than the dense tree sites. As discussed in the methods section some sensors malfunctioned later in the measuring campaign and the team used the opportunity to review some of the sites. The review found that due to limitations in installation some sensors were sited adjacent, but not immediately on the sites intended. This would explain results such as the ST1 and ST2 sites, where sensors were installed close to roadways and in parking lots adjacent to the site.

Table 3.1 – Results obtained from in-locisensors measuring air temperature and relative humidity, and derived heat index (August through October 2020). Mean and maximum conditions show that humidity levels play an important role in the sensation of heat.

	Local Climate Zone	Sensor	Mean			Maximum		
			Air Temperature	Relative Humidity	Heat Index	Air Temperature	Relative Humidity	Heat Index
Developed	Heavy Industrial	HI1	74.59	71.78	75.82	92.54	100.00	102.00
		HI2	76.11	66.68	77.35	97.81	97.36	103.00
	Compact Mid-Rise	CMR1	74.91	68.52	76.02	91.94	97.16	97.00
		CMR2	74.96	68.29	76.04	92.11	96.38	97.00
	Open Mid-Rise	OMR1	73.88	73.86	75.09	92.38	100.00	101.00
		OMR2	75.18	69.36	76.43	96.65	100.00	104.00
		OMR3	75.02	69.27	76.20	94.25	99.35	100.00
	Compact Low Rise	CLR1	75.20	68.74	80.41	94.39	99.78	101.00
		CLR2	74.76	69.84	80.07	96.65	100.00	101.00
	Open Low Rise	OLR1	74.58	70.63	80.13	93.69	100.00	100.00
		OLR2	73.99	73.03	79.74	93.1	73.03	97.00
		OLR3	73.87	72.00	80.17	92.13	100.00	100.00
OLR4		74.53	70.15	80.09	92.25	99.56	100.00	
Vegetated	Sparsely Built	SB1	73.76	71.83	80.37	93.56	100.00	100.00
	Low Plants	LP1	73.49	74.34	80.23	92.98	100.00	101.00
		LP2	73.23	76.46	81.10	94.39	100.00	105.00
	Scattered Trees	ST1	74.42	71.29	80.60	96.38	100.00	106.00
		ST2	74.29	71.14	75.44	93.69	100.00	102.00
	Dense Trees	DT1	71.66	79.13	72.75	89.23	100.00	96.00
	DT2	72.17	75.59	76.02	88.71	100.00	96.00	

Further investigation is needed to understand how wind speed and direction might be playing a role in cooling of sites, particularly CMR1 and CMR2, both situated close to the New Haven Green. Studies suggest that open space can contribute to ventilation and as a result aid in the dissipation of heat. It is unclear if this is the factor contributing to the readings obtained. However, the team also investigated previous meteorological data from the New Haven airport and developed a psychrometric chart to investigate what types of conditions contribute to cooling in the town. **Figure 3.5** shows the thermal sensation for a typical year in New Haven, based on the past 30 years of meteorological gathered from the airport’s weather station. For hot and humid days, the chart indicates that the best coping strategy

should be the promotion of natural ventilation. This result supported the team’s hypothesis that wind might be playing a role in the reduction of heat sensation in certain areas and the exacerbation of it in others. However, further investigation is needed to determine how wind circulation might be acting as a cooling strategy in the locations measured.

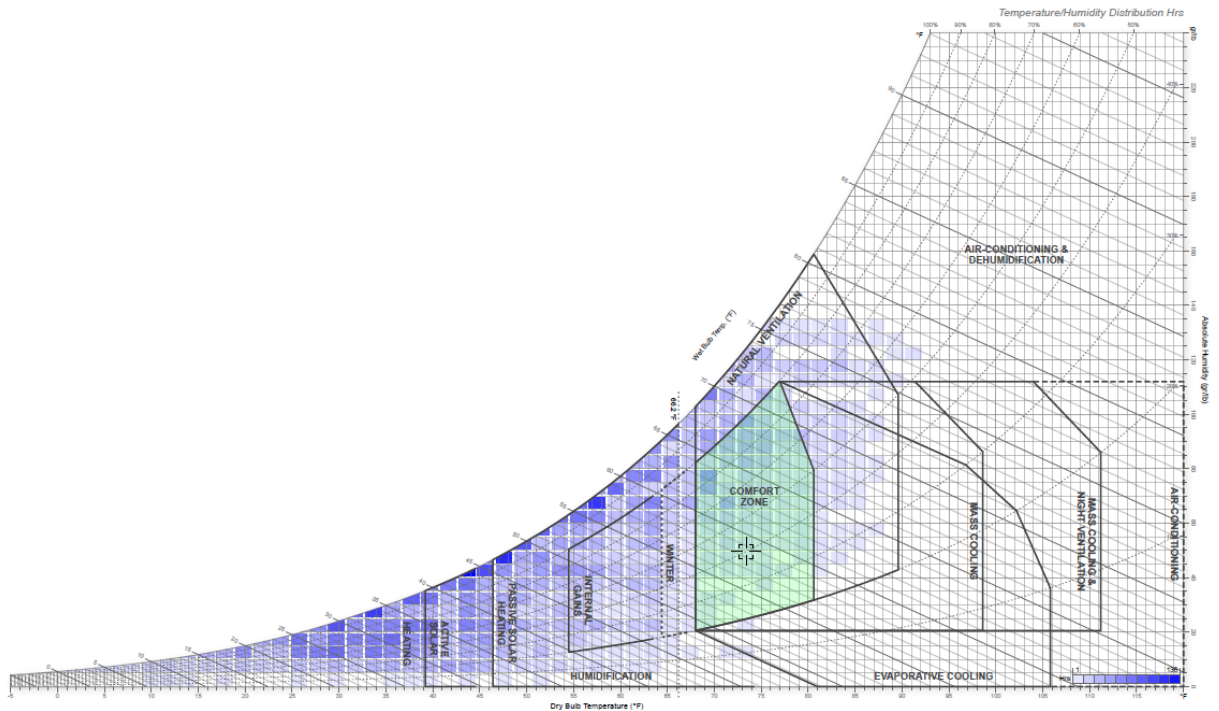
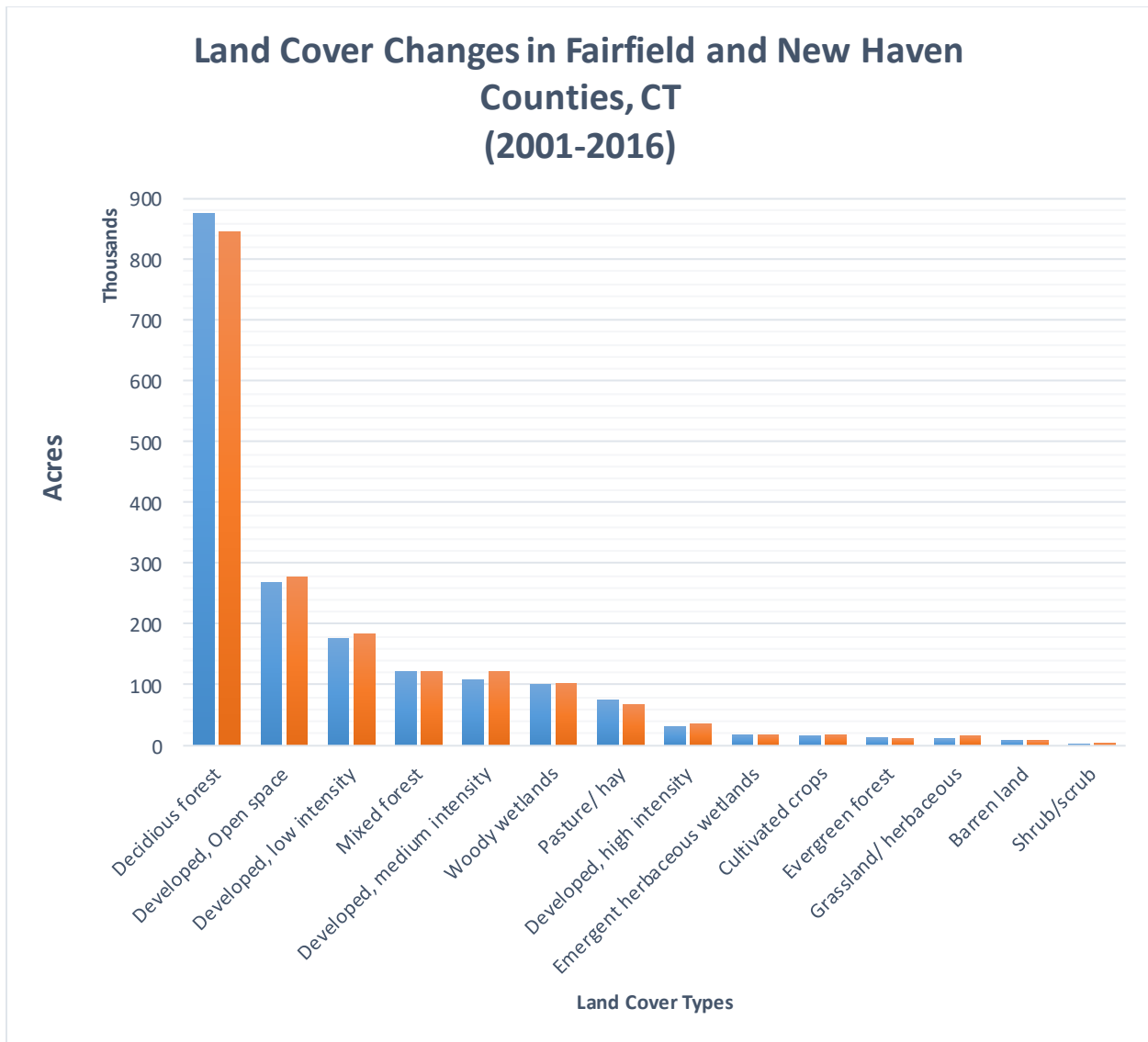


Figure 3.5 – Psychrometric chart developed based on meteorological data retrieved from the New Haven airport. Chart indicates the number of hours in a year that are in thermal comfort, cold stress, and heat stress, and the coping strategies. The chart indicates natural ventilation as the most effective solution for hot days in New Haven.

3.3. Long-term LULC Changes: National Land Cover Data Analysis

The first step in analyzing the retrieved land cover data was to understand the magnitude of changes in land cover types. As seen in Graph 3.1, the deciduous forest is the most representative land cover type within the study area throughout the study period. As seen in Table 1, deciduous forest corresponds to over 45% of the land coverage of the study area. The next most representative land cover type is developed, open space, which covers between 14.67% (2001) to 15.14% (2016) of the area.



Graph 3.1 - Total area of land cover type change between years ending in 2001 and 2016, ordered from most to least representative typologies.

Furthermore, Table 3.2 indicates that the greatest net gains in acreage were seen in the urbanized categories, particularly, developed, medium intensity (12,549 acres), open space (8,859 acres), and low intensity (7,904 acres). Based on the percentage the greatest gains were seen in less representative land cover types, such as shrub/scrub (36.99%), grassland/ herbaceous (29.75%), and developed, high intensity (13.33%). The greatest net losses were seen in deciduous forest (-30,073 acres) and pasture/ hay (-7,934 acres). The latter also saw the highest percentage of loss (-11.74%), followed by barren land (-6.63%), and evergreen forest (-4.93%).

Overall, the most representative land cover types were among the typologies that saw the greatest areal changes. It is important to point out that combined all the developed categories indicate a total gain of 34,031 acres of urbanized lands. In comparison, all three forested land cover types underwent losses,

summing a loss of approximately 31,138 acres within 15 years, though deciduous forests were by far the most impacted.

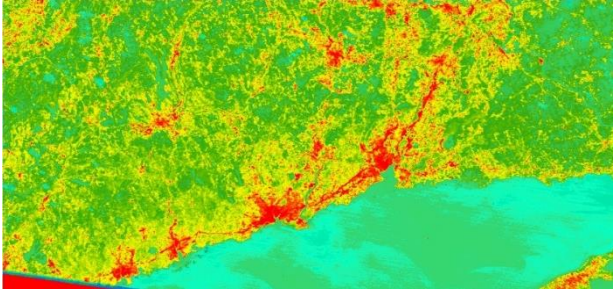
Table 3.2 - Changes in area per land cover type, indicating representation per study period and losses or gains over time.

NLCD Code	Land Cover Type	Total Area	% Total	Total Area	% Total	Loss/Gain	Percent loss/gain
		2001	2001	2016	2016		
41	Deciduous forest	876,425.75	47.86%	846,353.01	46.17%	-30,072.74	-3.55%
21	Developed, Open space	268,606.87	14.67%	277,465.97	15.14%	8,859.10	3.19%
22	Developed, low intensity	176,811.20	9.66%	184,715.74	10.08%	7,904.54	4.28%
43	Mixed forest	122,251.88	6.68%	121,794.17	6.64%	-457.72	-0.38%
23	Developed, medium intensity	108,793.40	5.94%	121,342.23	6.62%	12,548.84	10.34%
90	Woody wetlands	101,641.56	5.55%	102,205.76	5.58%	564.20	0.55%
81	Pasture/hay	75,508.42	4.12%	67,574.75	3.69%	-7,933.66	-11.74%
24	Developed, high intensity	30,677.84	1.68%	35,396.16	1.93%	4,718.32	13.33%
95	Emergent herbaceous wetlands	17,964.29	0.98%	17,814.23	0.97%	-150.05	-0.84%
82	Cultivated crops	16,866.12	0.92%	17,601.49	0.96%	735.37	4.18%
42	Evergreen forest	12,935.86	0.71%	12,328.09	0.67%	-607.77	-4.93%
71	Grassland/ herbaceous	11,008.96	0.60%	15,671.71	0.85%	4,662.74	29.75%
31	Barren land	8,708.16	0.48%	8,166.41	0.45%	-541.75	-6.63%
52	Shrub/scrub	2,979.26	0.16%	4,728.32	0.26%	1,749.06	36.99%
	Total area	1,831,179.58	1.00	1,833,158.05	1.00	1,978.47	

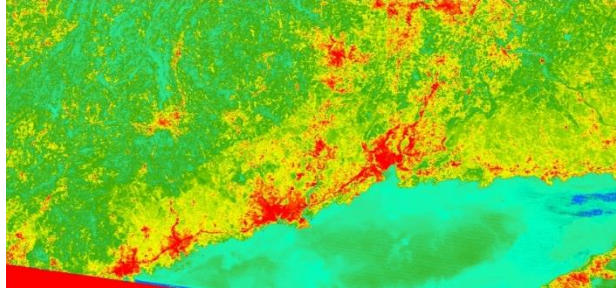
3.4. Long-term Land Surface Temperature Changes

As described in the methodology, land surface temperature changes were analyzed for 3-year intervals for the following study period, identified by the end year: 2001, 2006, 2011, 2016, 2020. The 20-year analysis of land surface temperature indicates that 2011 reached the hottest surface temperatures within the study period, as indicated in Figure 1. Further analysis regarding extreme weather events and weather patterns for the study period is presented in the statistics section, comparing the findings from the remote sensing analysis and air temperature data retrieved from the New Haven airport meteorological station.

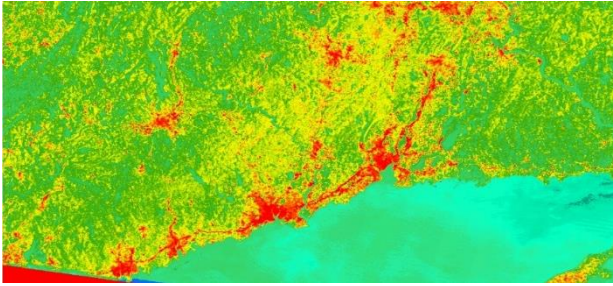
1999-2001



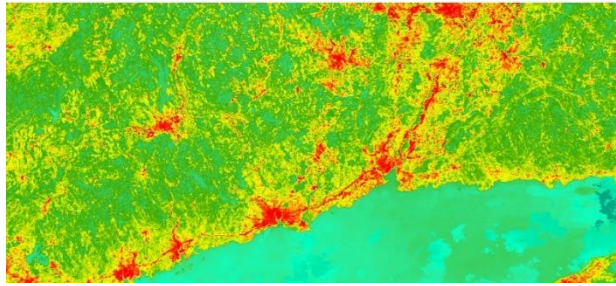
2004-2006



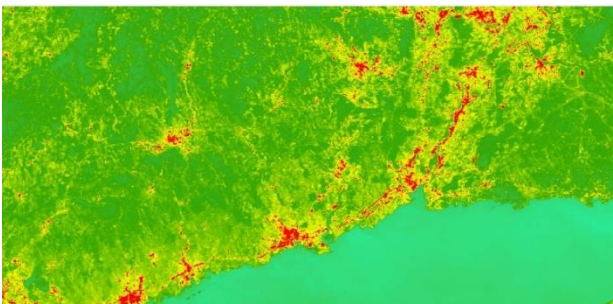
2009-2011



2014-2016



2018-2020



Maximum Surface Temperature

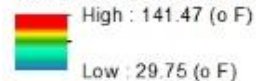


Figure 3.6 - Maximum surface temperature reached during each study period. Higher temperatures reached during 2009 to 2011 period. However, 2018 to 2020 period indicates new areas where temperatures heating has occurred.

Slope analysis of the maximum land surface temperature changes over time indicates the presence of warmer and cooler areas, as seen in Figure 2. Warming occurred primarily in western coastal towns, such as Greenwich, Stamford, New Canaan, Darien, and Norwalk, and north of New Haven, toward Hartford. In Fairfield County, Darien was the town with the highest warming, with a patch in the northeast part of the town warming on average 8 oF over 20 years. While Wolcott and Waterbury share an area that saw surface temperature increases of up to 9.25 oF. Cooling was seen along the shoreline of coastal towns from Westport to Madison, with significantly cooler areas present in Stratford. Fairfield county saw inland areas of cooling between Ridgefield and Sherman, however, the lowest surface temperatures were seen along the Stratford shoreline, with cooling of 7 oF on average. New Haven presented the most cooling in Milford, reaching approximately 8 °F lower temperatures than seen during the 2001 study period.

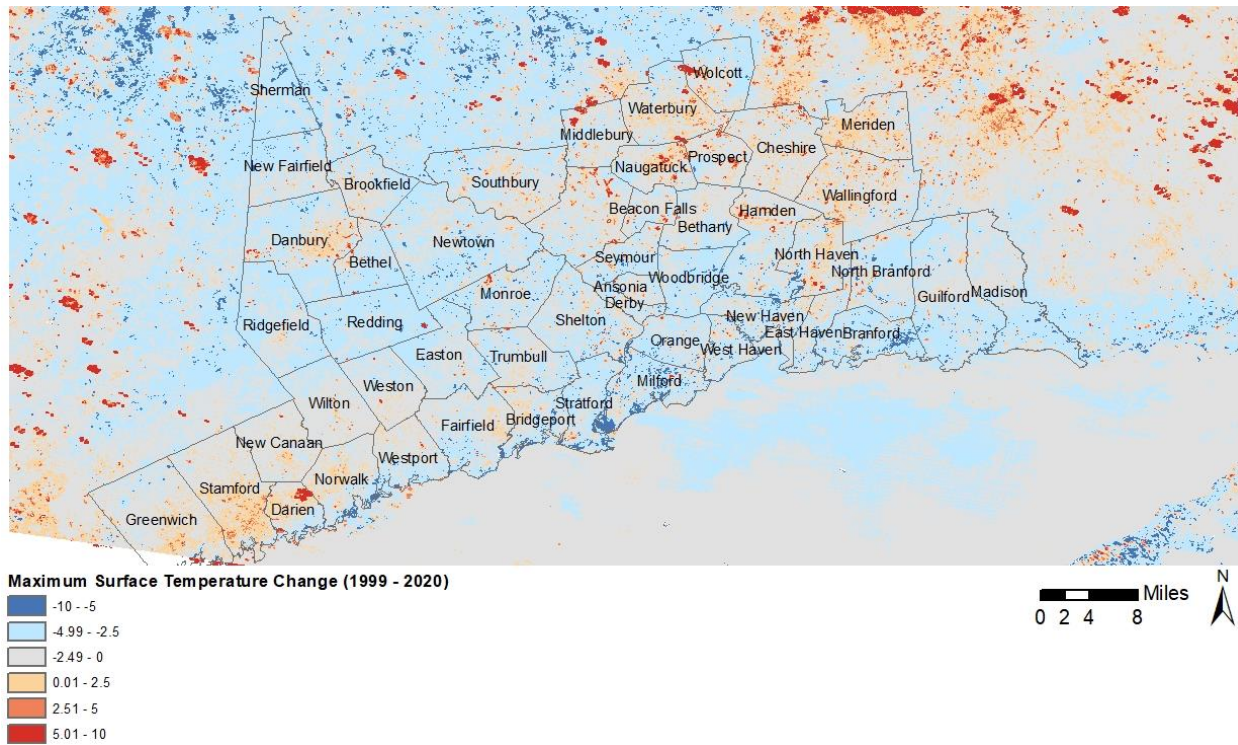
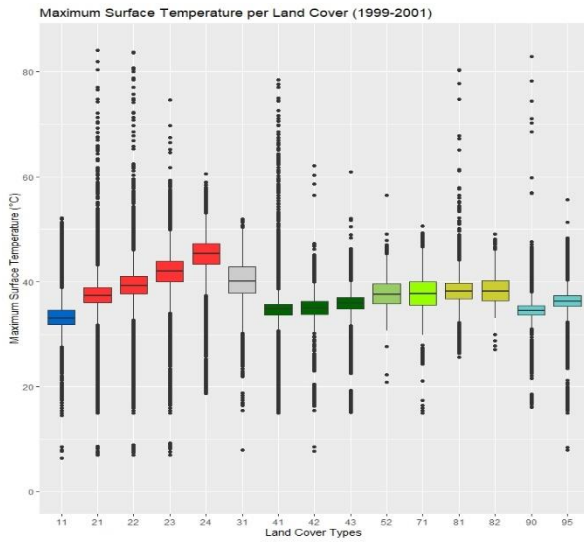


Figure 3.7 – Maximum surface temperature change between 1999 to 2020 in Fairfield and New Haven counties, CT. Map shows areas with temperature increases and decreases of up to 10 degrees Fahrenheit. Cooling areas were seen in the coast near the water, while areas with temperature increases were in western Fairfield and northeastern New Haven.

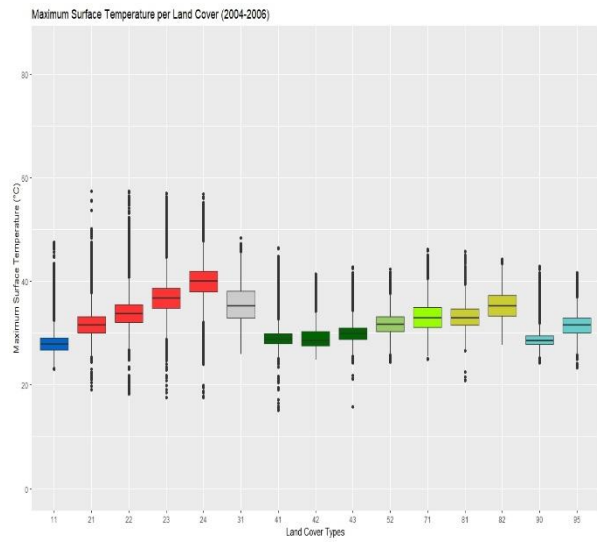
3.5. Relationship Between LULC Changes and LST Changes Over Time

The team applied a statistical analysis to interpret the relationship between changes in LULC and LST. This phase first focused on comparing the average maximum surface temperature reached by each land cover type for each study period. As shown in Graph 3.2, the 1999 to 2001 data showed a higher spread of temperature, with a larger number of outliers both for high and low temperatures. This data also reiterated observations made in the mapping section, indicating that study periods ending in years 2001 and 2011 reached higher averages for all land cover categories when compared to those ending in years 2006 and 2016. Overall, all three study periods displayed a very similar pattern with developed land covers consistently reaching higher temperatures. Moreover, the variation among developed types was consistent throughout, with the same magnitude of change in all four study periods, and higher temperatures seen in order from high intensity to open space developed typologies.

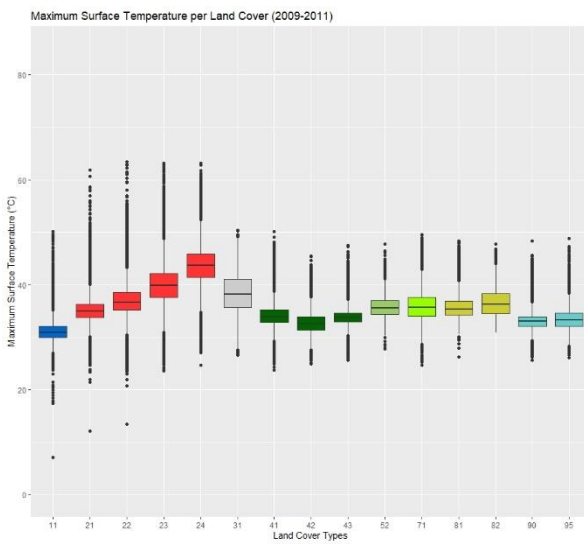
1999-2001



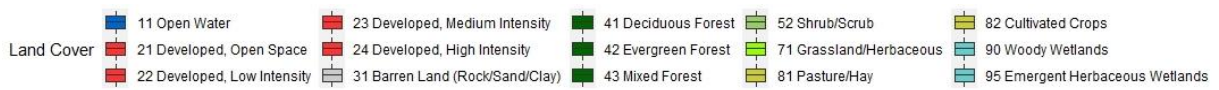
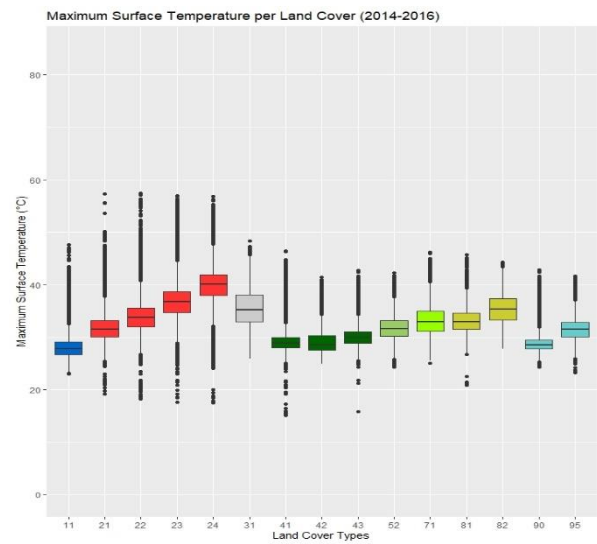
2004-2006



2009-2011



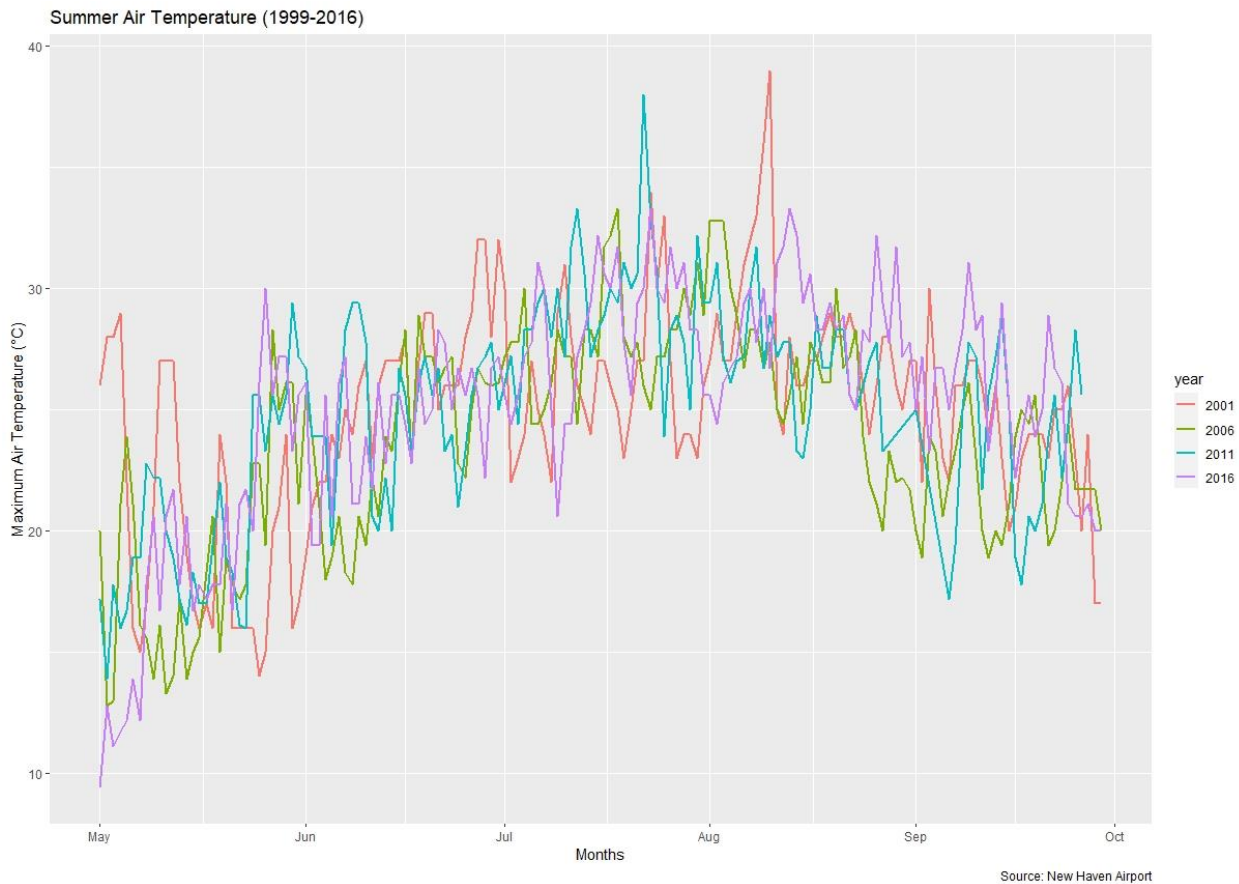
2014-2016



Graph 3.2 - Boxplot analysis of maximum surface variation per land cover type per study period.

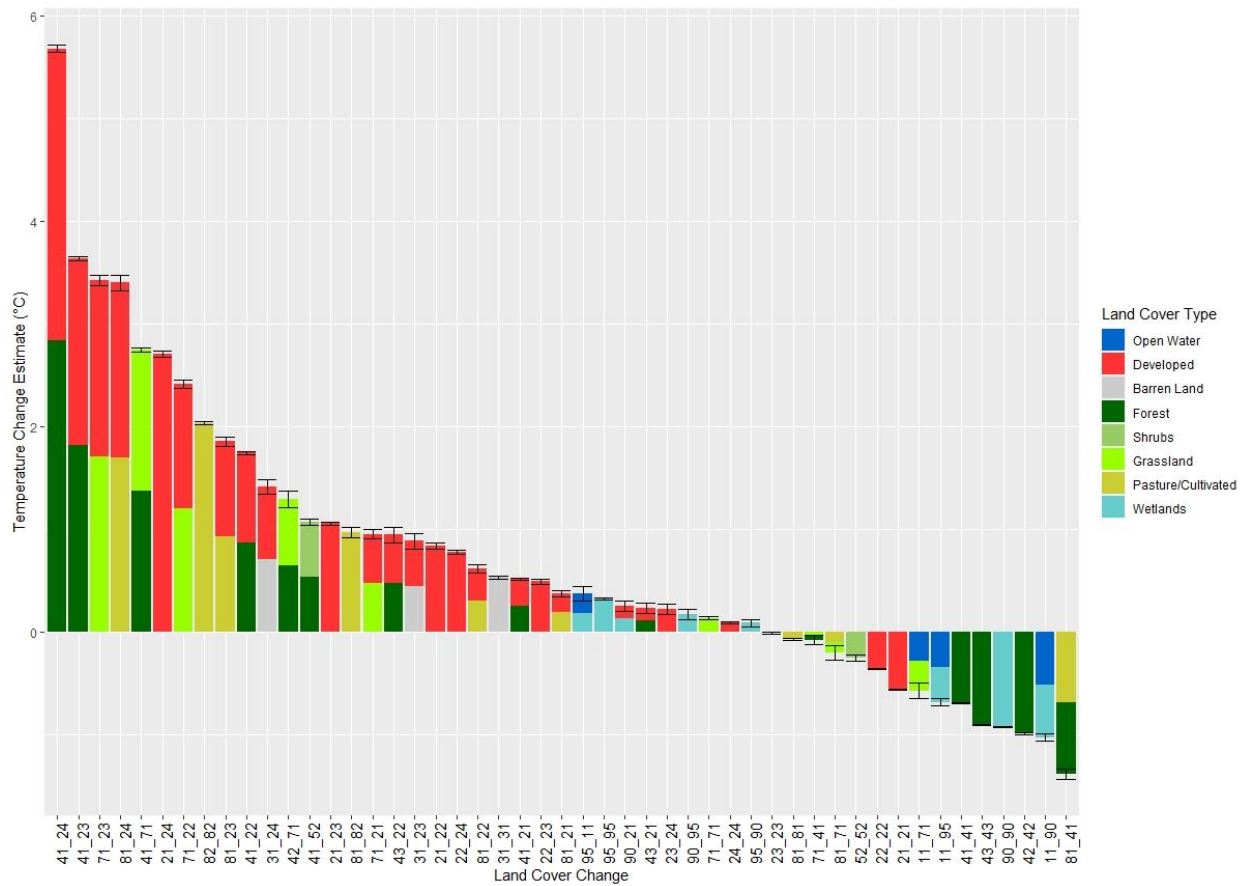
Data from the New Haven airport meteorological station was retrieved to better understand the surface temperature fluctuations seen in the surface temperature data for each study period (Graph 3.3). The data retrieved focused on the maximum air temperatures reached during the months of May through September of each year. Similar to the patterns seen in the remotely sensed data, air temperature data indicates that 2001 and 2011 were the years with highest temperature spikes. In fact, according to the National Weather Service, Fairfield and New Haven counties underwent 2 heat days during the 1999 to 2001 period, 1 during the 2004 to 2006 period, 1 excessive heat day during the 2009 to 2011 (record high heat index reached in this station to date), and finally 1 excessive heat day in 2014 to 2016. More

importantly, though all of the study periods faced hot periods, the spikes in the 2001 and 2011 ending study periods confirm the data retrieved from the satellite images and give a better indication of the variability that occurred within the 15 years analyzed.



Graph 3.3 - Comparative maximum air temperature from May through September for each study period. Source: New Haven airport meteorological station.

A linear regression was then applied to the combined LST and NLCD datasets (Graph 3.4). The statistical model accounts for the variability during the study period and ranks temperature changes based on the average temperature changes seen between the 15 years sampled, based on land cover changes. Graph 3.4 shows that independently of 2016 being slightly cooler than 2001, overall changes from vegetated land covers to developed land covers resulted in increases to land surface temperatures. On the other hand, cooler temperatures resulted from unchanged land cover or variations within vegetated land covers. By far the most intense temperature increases occurred from deciduous forest (41) to developed, high intensity (24) which resulted in the highest temperature changes, estimated at approximately 5.5 oC (9.9 oF). Loss of forest cover was consistently linked to increase in temperature, as well as intensification of development. The most curious findings were the reduction of temperature for unchanged open space and low intensity development. Further study inquiring is needed to identify the type of vegetation present in these types of development. As seen with the use of the LCZ classification, in Phases 1 and 2, Fairfield and New Haven counties have a considerable amount of tree canopy cover within residential properties. The findings from this phase could be hinting at the role of trees and vegetation as cooling mechanisms within low intensity development.



Graph 3.4 - Temperature variation estimates based on the average temperature changes between 1999 to 2016.

4. Conclusion and Recommendations

Overall, this study indicates that both Fairfield and New Haven counties have suffered losses of important vegetated ecosystems in the last 15 years. There are clear indications that urban heat islands are occurring, and surfaces are hotter over the last 20 years. Yet the results also indicate that a significant amount of critical landscapes remains, such as deciduous forest covers, that need to be preserved to ensure heat adaptation.

The short-term analysis produced indicates that much of the dense canopy cover in the counties seems to be in properties classified as sparsely built. These are mostly residential areas, suggesting that forested areas are within private properties. As seen during this phase, sparsely built development (LCZ) or developed, low intensity (NLCD) has intensified over the last 5 years. The appearance of this classification seems to be the first indication of sprawl in some towns, followed by further intensification with categories such as open low rise or open midrise (developed, medium intensity) and compact low rise or compact midrise (developed, high intensity). With that in mind, it is important to further understand if the trends seen in the last 5 years will continue.

Recommendations based on this phase are:

1. Communicate and propose strategies that conserve tree canopy cover within public and private properties.

Plans of conservation and development should address localized incentives and approaches to protect existing tree canopy cover. To do so further inquiring is needed on how plans of conservation and development currently promote development in these areas. Furthermore, it is important to understand and establish how greenspace is conserved and how vegetation clearing managed in private properties at the municipal level. This information could guide a statewide decision-making approach towards conservation of vegetation to ensure the maintenance of greening.

2. Promote the shift from Euclidean land-use planning to Form-based planning practices

The use of the LCZ classification hints to the diversity of urban environments that exist in both counties, which do not respond to climate in the same way. As previously mentioned, this classification is modeled after design and planning fields and points to the need for decision-making that interprets our environments in a more holistic view, rather than strictly use-based. This suggests a needed move toward form-based planning codes rather than traditional Euclidean land-use planning codes that focus mostly on land-use rather than considering the three-dimensional aspects of our environments. The short-term analysis shows the diversity of urban environments present in both counties. Furthermore, though limited, the findings from the sensor network point to how vegetation and potentially ventilation could play a role in heat adaptation. The variation between heat and humidity levels indicate that some urbanized areas adapt better to higher temperatures than others. Though further inquiry is needed to understand the role of ventilation, the classification based on land-use limits decision-makers' ability to think about how to better design our cities. The city of New Haven has already made advancements in this direction. The city's Vision 2025 discusses the incorporation of form-based code standards to improve site design, furthermore, the New Haven City Plan office has already begun to explore the application of form-based code to address climate adaptation and sustainability (New Haven Vision 2025 2015).

The long-term analysis presented in this study indicate cooling in areas where vegetation cover increased. In the meantime, intensification and expansion of urban heat islands occurred in the western portion of Fairfield and inland in both counties due to development intensification in the last 20 years. The study also highlights that there is a critical mass of existing forested and vegetation covers in the state that seem to aid in cooling. However, further research needs to be done to understand the applicability and incorporation of heat response planning in plans of conservation and development. Studies in urban climatology suggest that urban heat island mitigation and adaption relies in the presence of contiguous greening (Debbage and Shepherd 2014). Therefore, we need to understand how the trends seen correspond to policies and town planning codes to better outline plans that support contiguous green infrastructure within the counties.

Recommendations based on this phase are:

3. Promote the inclusion of heat response planning as a component of plans of conservation and development.

Plans currently recognize the impacts of water-related hazards, however, heat has overlapping design and planning considerations that could lead to adequate multi-hazard adaptation. As indicated by this

study vegetation, similar to flood adaption, is key to promoting heat response. Therefore, towns should promote the inclusion of green space as a way of supporting healthy communities. Moreover, greening should not be seen as limited to pockets of the town, but rather as the establishment and maintenance of networks of greenspace. This is beneficial for promoting permeability and ensuring that greening occurs continuously will support not only healthier communities, but healthier ecosystems.

Finally, further investigation is needed to understand the rest of the state's LULC and LST conditions. This study suggests that 'heat corridors' might be occurring along major highways and connecting to major cities in the state. For instance, the long-term analysis indicated heating toward the city of Hartford, yet the state's capital is not contemplated in this study. Furthermore, it is unclear if the trends seen in both Fairfield and New Haven counties are similar in the rest of the state.

Additional recommendation:

4. Expansion of short-term and long-term analysis of heat to the entire state of Connecticut

In the short-term additional towns need to be sampled to understand the localized relationships between air temperature, relative humidity, and wind. Strategies for adapting to heat, as shown in the psychrometric chart for New Haven, will likely vary for inland towns, therefore, wind might not play as strong role in adaptation as it might in coastal cities. A network of sensors could support localized decision-making that supports greening and permeability. The long-term analysis will better aid in the comprehension of 'heat corridors' and help decision-makers determine areas that require conservation or expansion of greening. Cities such as Hartford and New Haven have already begun efforts to improve urban greening, however, a larger study such as this one could support cross-municipal efforts that strive to improve heat response at a larger scale.

5. Glossary of Terms Used

Fraction of Vegetation Cover (FVC) → the percentage of the ground cover that is composed of green vegetation compared to the total studied area. This varies seasonally, as some species of trees and plants lose their leaves during the colder months (late-Fall, Winter, and early-Spring), exposing barren and developed surfaces beneath them.

Heat Index → a measurement that combines the effects of temperature and humidity of the air to estimate the average person's level of discomfort during hot days.

Land Surface Temperature → the sensation of how hot or cold a surface of the Earth is to the touch.

Normalized Difference Vegetation Index (NDVI) → is an index derived from satellite images that quantifies vegetation density and allows us to evaluate changes to plant health over time. NDVI maps depict the calculated ratio between red and near infrared bands. Health vegetation shows a high reflectance of near infrared and low reflectance of red. Therefore, areas that display high reflectance of red are typically not vegetated and associated with developed and barren landscapes.

Psychrometric Chart → a graphic representation of the relationships between temperature and humidity to identify environmental issues and assess design solutions.

Remote Sensing → is the technique of acquiring information from a distance. In this study, it refers to information captured by sensors installed on satellites that can detect energy reflected or emitted from the Earth's surface.

Surface Emissivity → a metric to determine how much heat is emitted by a surface.

Urban Heat Island (UHI) → refers to urban environments that are warmer than its surrounding, which are typically rural or less developed areas. Urban structures, such as buildings and roads, along with certain human activities, can absorb and re-emit the sun's heat and sometimes even produce heat. Dense urban environments produce more heat than natural landscapes, which results in clusters or islands of hotter areas relative to vegetated and less dense surroundings.

6. References

Aniello, C., Morgan, K., Busbey, A., Newland, L., 1995. Mapping micro-urban heat islands using Landsat TM and a GIS. *Comput. Geosci.* 21, 965–969.

Bechtel, B., Alexander, P.J., Beck, C., Böhner, J., Brousse, O., Ching, J., Demuzere, M., Fonte, C., Gál, T., Hidalgo, J. and Hoffmann, P., 2019. *Urban climate*, 27, pp.24-45.

Bozzi, L. ed., 2020. Extreme Heat in Connecticut: A Yale Center on Climate Change and Health Issue Brief. Yale Center on Climate Change and Health. Available at: https://ysph.yale.edu/yale-center-on-climate-change-and-health/policy-and-public-health-practice/YCCCH%20Extreme%20heat%20issue%20brief_407652_48542_v2.pdf [Accessed October 2021].

- Buyantuyev, A., Wu, J., 2010. Urban heat islands and landscape heterogeneity: linking spatiotemporal variations in surface temperatures to land-cover and socioeconomic patterns. *Landsc. Ecol.* 25, 17–33. <https://doi.org/10.1007/s10980-009-9402-4>
- Carlson, T.N. and Ripley, D.A., 1997. On the relation between NDVI, fractional vegetation cover, and leaf area index. *Remote sensing of Environment*, 62(3), pp.241-252.
- Ching, J., Mills, G., Bechtel, B., See, L., Feddema, J., Wang, X., Ren, C., Brousse, O., Martilli, A., Neophytou, M. and Mouzourides, P., 2018. WUDAPT: An urban weather, climate, and environmental modeling infrastructure for the anthropocene. *Bulletin of the American Meteorological Society*, 99(9), pp.1907-1924.
- Ermida, S.L., Soares, P., Mantas, V., Götsche, F.M. and Trigo, I.F., 2020. Google earth engine open-source code for land surface temperature estimation from the landsat series. *Remote Sensing*, 12(9), p.1471.
- Day, K., 2021. WUDAPT Level 0 training data for New Haven, CT (United States of America), submitted to the LCZ Generator. This dataset is licensed under CC BY-SA. Available at: https://lcz-generator.rub.de/factsheets/23b27de4751248875d01835c1fa82290c20b8758/23b27de4751248875d01835c1fa82290c20b8758_factsheet.html
- Debbage, N., Shepherd, J.M., 2015. The urban heat island effect and city contiguity. *Comput. Environ. Urban Syst.* 54, 181–194.
- Dousset, B., Gourmelon, F., 2003. Satellite multi-sensor data analysis of urban surface temperatures and landcover. *ISPRS J. Photogramm. Remote Sens.* 58, 43–54. [https://doi.org/10.1016/S0924-2716\(03\)00016-9](https://doi.org/10.1016/S0924-2716(03)00016-9)
- Dousset, B., Gourmelon, F., Laaidi, K., Zeghnoun, A., Giraudet, E., Bretin, P., Mauri, E., Vandentorren, S., 2011. Satellite monitoring of summer heat waves in the Paris metropolitan area. *Int. J. Climatol.* 31, 313–323.
- Fu, P., Weng, Q., 2016. A time series analysis of urbanization induced land use and land cover change and its impact on land surface temperature with Landsat imagery. *Remote Sens. Environ.* 175, 205–214. <https://doi.org/10.1016/j.rse.2015.12.040>
- Huang, M., Gao, Z., Hu, F., Wang, L., Miao, S., Li, J., Chen, F., LeMone, M.A., 2017. Estimate of Boundary-Layer Depth Over Beijing, China, Using Doppler Lidar Data During SURF-2015. *Bound.-LAYER Meteorol.* 162, 503–522.
- Hulley, G.C., Hook, S.J., Abbott, E., Malakar, N., Islam, T. and Abrams, M., 2015. The ASTER Global Emissivity Dataset (ASTER GED): Mapping Earth's emissivity at 100 meter spatial scale. *Geophysical Research Letters*, 42(19), pp.7966-7976.
- Johnson, D.P., Wilson, J.S., 2009. The socio-spatial dynamics of extreme urban heat events: The case of heat-related deaths in Philadelphia. *Appl. Geogr.* 29, 419–434.
- Johnson, D.P., Wilson, J.S., Luber, G.C., 2009. Socioeconomic indicators of heat-related health risk supplemented with remotely sensed data. *Int. J. Health Geogr.* 8, 57.
- Malakar, N.K., Hulley, G.C., Hook, S.J., Laraby, K., Cook, M. and Schott, J.R., 2018. An operational land surface temperature product for Landsat thermal data: Methodology and validation. *IEEE Transactions on Geoscience and Remote Sensing*, 56(10), pp.5717-5735.

- Mitraka, Z., Chrysoulakis, N., Kamarianakis, Y., Partsinevelos, P. and Tsouchlaraki, A., 2012. Improving the estimation of urban surface emissivity based on sub-pixel classification of high resolution satellite imagery. *Remote Sensing of Environment*, 117, pp.125-134.
- Miller, T., 2021. WUDAPT Level 0 training data for Bridgeport, CT (United States of America), submitted to the LCZ Generator. This dataset is licensed under CC BY-SA. Available at: https://lcz-generator.rub.de/factsheets/674d2ac43dcdf8565660c80bbf2caafe725fc718/674d2ac43dcdf8565660c80bbf2caafe725fc718_factsheet.html
- New Haven Vision 2025. A Plan for a Sustainable, Healthy, and Vibrant City (Plan of Conservation and Development), 2015. New Haven, Connecticut. Available at: <https://www.newhavenct.gov/civicax/filebank/blobdload.aspx?blobid=25816>.
- Parastatidis, D., Mitraka, Z., Chrysoulakis, N. and Abrams, M., 2017. Online global land surface temperature estimation from Landsat. *Remote sensing*, 9(12), p.1208.
- Rothfus, L.P. and Headquarters, N.S.R., 1990. The heat index equation (or, more than you ever wanted to know about heat index). *Fort Worth, Texas: National Oceanic and Atmospheric Administration, National Weather Service, Office of Meteorology*, 9023.
- Stewart, I.D. and Oke, T.R., 2012. Local climate zones for urban temperature studies. *Bulletin of the American Meteorological Society*, 93(12), pp.1879-1900.
- Stewart, I.D., Oke, T.R. and Kravynhoff, E.S., 2014. Evaluation of the 'local climate zone' scheme using temperature observations and model simulations. *International journal of climatology*, 34(4), pp.1062-1080.
- Voogt, J.A., Oke, T.R., 2003. Thermal remote sensing of urban climates. *Remote Sens. Environ.* 86, 370–384. [https://doi.org/10.1016/S0034-4257\(03\)00079-8](https://doi.org/10.1016/S0034-4257(03)00079-8)
- Weng, Q., Lu, D., Schubring, J., 2004. Estimation of land surface temperature–vegetation abundance relationship for urban heat island studies. *Remote Sens. Environ.* 89, 467–483.
- Weng, Q., Quattrochi, D.A., 2006. Thermal remote sensing of urban areas: An introduction to the special issue. *Remote Sens. Environ.* 2, 119–122.
- Yuan, F., Bauer, M.E., 2007. Comparison of impervious surface area and normalized difference vegetation index as indicators of surface urban heat island effects in Landsat imagery. *Remote Sens. Environ.* 106, 375–386.
- Zhou, W., Qian, Y., Li, X., Li, W., Han, L., 2014. Relationships between land cover and the surface urban heat island: seasonal variability and effects of spatial and thematic resolution of land cover data on predicting land surface temperatures. *Landsc. Ecol.* 29, 153–167. <https://doi.org/10.1007/s10980-013-9950-5>